國立臺灣大學理學院大氣科學研究所

碩士論文

Department of Atmospheric Sciences

College of Science

National Taiwan University

Master Thesis

弱縱觀天氣強迫與 PM2.5 濃度改變下台北盆地夏季午後強降水事件之合成分析研究

A Composite Analysis of Summer Afternoon Heavy Precipitation Events in the Taipei Basin Under Weak Synoptic Forcing and PM2.5 Changes

冉心瑩

Cidny A. Ramirez

指導教授：楊明仁 博士

Advisor: Ming-Jen Yang Ph.D.

中華民國 112 年 7 月

July 2023

ABSTRACT

Taipei, Taiwan is a city affected by various types of precipitation. However, one of the most impactful short-term sources of precipitation is afternoon thunderstorms. Understanding the trends of these afternoon thunderstorms and the extent to which PM2.5 impacts precipitation totals is imperative for improving forecasting and developing urban infrastructure that can deal with said totals.

The present study looks at the top 5% heavy rain (HR) events in the Taipei Basin during the summer months of June, July, and August from 2005 to 2015. The goal was to find out whether changes in the PM2.5 concentration over the Taipei Basin has had any impact on HR events in the summer months. The total PM2.5 concentration during the same period was analyzed and compared to various characteristics of the HR events. Heavy rain events were defined as having a total rainfall of at least 81.24 mm/day and occurred in a weak synoptic environment. 55 days met the criteria. The rainfall during each day was then analyzed by its temporal and spatial distribution. Rainfall trends were compared to PM2.5 trends. Spatial and temporal analyses of PM2.5 trends for the summer season and each of the HR days were used for comparison. A background summer mean was computed for the decade (2005-2015) and was used as a constant background state value to compare the daily concentration fluctuations. It was found that in only some events the PM2.5 concentrations responded actively to precipitation. Overall concentrations on HR days did not vary significantly from the summer mean.

Further, three rainfall case studies were selected: a Mei-Yu event, a single HR day, and three consecutive HR days. The day before the HR event and the day after were included in the analysis for each case study. The case studies only provided insight into the effect that rainfall has on PM2.5 concentrations but not into the effect that PM2.5 may have on rainfall.

NTU WRF-ARW was used to simulate various PM2.5 concentrations (*clean, average, dirty*) and see if precipitation spatial and temporal characteristics varied. Changes in aerosol concentrations affected precipitation. The changes were reflected by changes in the timing (initiation and duration) and distribution (location of heaviest rainfall) of the rain. PM2.5 likely affected the microphysics of the storm cloud development, changing the initial conditions for the storm itself. While the exact way that PM2.5 influences HR development is unknown, it is clear that increased concentrations affect rainfall rates in the Taipei Basin.

ACKNOWLEDGEMENTS

I would like to thank everyone who has made this journey possible. It was not an easy journey, but with support, food, and tissues here we are today. Thank you to my parents and sister, and my extended chosen family. Thank you to my UAlbany advisors Christopher Thorncroft and Ryan Torn, and my NTU advisor Ming-Jen Yang.

Thank you, Taiwan, for showing me what beauty, love, happiness, and good food is.

CONTENTS

LIST OF FIGURES

LIST OF TABLES

LIST OF ABBREVIATIONS

in alphabetical order

ARMTS	Automatic Rainfall and Meteorological Telemetry System
CCN	Cloud Condensation Nuclei
CWB	Central Weather Bureau
EPA	Environmental Protection Agency
GFS	Global Forecasting System
HR	Heavy Rainfall
JJA	June, July, August
JMS	Japan Meteorological Society
LST	Local Standard Time
LWC	Liquid Water Content
MCS	Mesoscale Convective System
NCEI	National Centers for Environmental Information
NOAA	National Oceanic and Atmospheric Administration
GIBBS	Global ISCCP B1 Browse System
NTU	National Taiwan University
PBL	Planetary Boundary Layer
PM	Particulate Matter
PM10	Particulate Matter of 10 Micrometers of Less
PM2.5	Particulate Matter of 2.5 Micrometers of Less
TCCIP	Taiwan Climate Change Projection and Information Platform
UHI	Urban Heat Island

WRF	Weather Research and Forecasting (model)
WRF-ARW	Weather Research and Forecasting (model) - Advanced Research WRF

1 Introduction

Precipitation is crucial to the successful development of any society, as it provides for the basic necessities of mankind, from refilling reservoirs to irrigating crops. However, heavy precipitation events can bring disaster in the form of floods, loss of life, and property damage, making these events crucial for scientific study. Heavy precipitation events can have various causes, and while most people associate them with tropical storms (hurricanes, typhoons, and cyclones) and monsoons, more localized small-scale events such as thunderstorms can also produce large precipitation amounts and flash flooding. Understanding the factors that contribute to the development of heavy precipitation producing thunderstorms is crucial to the development of societies, such as Taipei, Taiwan, which are affected by such storms. Studying and understanding these phenomena can lead to advancements in forecasting and better preparation to handle large amounts of precipitation. In this case, in Taipei, urban development and plans to change land use can lead to modifications to the surface permeability, water flow, and drainage so that when these heavy precipitation events do occur, the amount of property damage and business closures are minimal. One of the factors that can affect the habits of heavy precipitation events is aerosol emissions, specifically PM2.5. This study looks at how changes in the PM2.5 concentration in the Taipei Basin have impacted heavy rainfall events in the summer months.

As a small island between East Asia and the greater Pacific region, Taiwan is affected by several different large-scale weather patterns that govern precipitation distribution and amounts, including the East Asian summer monsoon, the Mei-Yu/ Bai Yu front, and typhoons. Even though the summer is considered a dry season in northern Taiwan, maximum rainfall in the Taipei Basin occurs in the summer. This is due to frequent summer afternoon thunderstorms accounting for 75% of the total summer rainfall in the basin (Chen et al. 2007), (Chen et al.

2016). The Taipei Basin is an important area because it includes Taipei, the capital of Taiwan and its largest city, making it an economic and political powerhouse. Over the years, there has been extensive urbanization in the basin. Since the 1960s, the population has increased by a factor of 3.5 to reach 7.4 million, with nearly a third of the nation's population living in this urban area. In addition, urbanized land cover has increased by close to a factor of 3 since the 1960s (Chen et al. 2007; World Population Review, 2015).

The Taipei Basin is a geographically unique area to study thunderstorms. It is nestled between Yangming Mountain in the northeast and part of the Snow Mountain Range in the south and the Keelung and Tamsui River valleys, which provide river flow to and from the Pacific Ocean. Due to urbanization, not only has land surface changed in the basin, but air quality has changed as well. Particulate matter of 2.5 micrometers or less in diameter, otherwise known as PM2.5, is a commonly discussed particle in the realm of air pollution. Such tiny particulates can come from chemical reactions that occur in the atmosphere and form sulfur dioxide and nitrogen oxides emitted from automobiles, power plants, and other industries (EPA, 2021). Much of the general public's concern about PM2.5 regards public health and most people relate PM2.5 to haze. It is also important to understand how such particulates impact precipitation tendencies and to examine whether the urbanization that Taipei has experienced has in fact played a role in the changes of afternoon thunderstorms as Chen et al. (2007) suggests. Chen et al. (2007) also reported an increase in thunderstorm activity and rainfall during the past four decades. A combination of PM2.5 and thunderstorm activity presents issues for the basin as changes in land surface, and rainfall can affect the water supply, ground subsidence, urban planning, pollution, and air and land traffic hazards (Chen et al. 2016). While there have been many studies on these

afternoon thunderstorms, it is essential to understand the nature of these extreme events since they are the ones that pose the greatest risk to city infrastructure.

1.1 Afternoon Thunderstorm Conditions

Thunderstorms in the Taipei Basin can be classified as airmass thunderstorms, forming in the presence of four key ingredients: elevated moisture and instability, orography (high mountains), and heating (from the urban Taipei setting). Mountains, valleys, land-sea breeze circulation, and the urban heat island (UHI) effect are all features that satisfy the airmass thunderstorm criteria and are all found in the basin. Lin, P., et al. (2011) looked at some of these features and how they impacted the thermodynamic mechanisms of thunderstorm days during the warm season from 2005-2008 under weak synoptic forcing. From the statistical analysis of surface stations, rain gauges, and soundings, the authors found that compared to non-thunderstorm days, the pre-convective environment on thunderstorm days is warmer and moister near the surface with an excess of 0.5ºC in mean temperature and an excess 1.0ºC in mean dewpoint. At mid-levels (750-550 hPa), non-thunderstorm days were also, on average 2.5-3.5ºC drier than thunderstorm days based on dew point comparisons. Lin, P., et al. (2011) agrees with Fuelberg and Biggar (1994). While studying the pre-convective environment of summer thunderstorms in Florida, Fuelberg and Biggar (1994) found that days with strong convection tend to be moister at mid-levels. They also found that while both thunderstorm and non-thunderstorm days have southwesterly winds, they are stronger on thunderstorm days and likely bring in relatively warmer and moister air masses. This creates favorable conditions for thunderstorm development by increasing instability and decreasing the possibility for dry air entrainment at mid-levels.

While Lin, P., et al. (2011) touched on some of the synoptic conditions that play a role in the development of thunderstorms in the Taipei Basin, Chen et al. (2016) did a more in-depth analysis in an effort to improve the forecasting of said thunderstorms, building on the observational study that Chen et al. (2014) presented. The authors expanded the study dates from Chen et al. (2014) to a seven-year period of 2007-13 to have a larger sample size. Their study found that the synoptic conditions on thunderstorm days are characterized by a weak northwest-southeast ridge around the northern section of Taiwan, with a surface low over Indochina and a high over the Philippine Sea. This synoptic structure is favorable to convective development, as the ridge that passes over Taiwan transports warm, moist air to the Taipei Basin. Morning soundings from Banqiao (Figure 1) further support this idea, as thunderstorm days have a lower dewpoint depression both at the surface and at 500 hPa than non-thunderstorm days. A composite of the winds using the same soundings shows that on thunderstorm days at 700 hPa, the winds are about 6.0 m/s southwesterly compared to 4.2 m/s southeasterly on non-thunderstorm days, similar to Lin, P., et al. (2011) finding that southwesterly winds are more pronounced on thunderstorm days.

To build on existing research on the dynamics of afternoon thunderstorms and previous field experiments in the Taipei Basin, Miao and Yang (2020) used an observational case study from June 14, 2015, to analyze land-sea breeze circulation as well as topography and microphysics. Observation studies show that most thunderstorms in northern Taiwan start off on the mountain tops and move downslope, where storm outflow can collide with sea breezes around the Taipei Basin, so Miao and Yang (2020) used the Weather Research and Forecasting (WRF) model to fill the gaps that observation studies left. They found that while the mountains to the south of the basin provide a birthplace for thunderstorms, the mountains to the north have

valleys intensify the sea-breeze circulation and the moisture supply to the basin, which aids convective development. In other words, once a thunderstorm develops and moves downhill into the basin, its cold pool collides with the moisture carried by the sea breeze. This increased thermodynamic instability produced enhanced low-level convergence, lifted parcels, and further fueled thunderstorm development.

Sea-breeze circulation presents itself as a key factor in the mesoscale development of thunderstorms due to the moisture they can provide to fuel precipitation, so it is something that we must define. Land-sea breeze circulation occurs due to the thermal contrast between land and sea. Soil has a lower heat capacity than air and water, so as the sun rises and sets, a differential in heating/ cooling rates creates a circulation pattern. During the day, when the soil is hotter, air rises over the land and sinks over the water creating a breeze from the water towards land, known as a sea breeze. After sunset, since the land cools faster than water, the warmer air rises over the water and sinks over the land creating a breeze from the land to the water, known as a land breeze (NBDC, NOAA; L. Zhu, 2017). On days that have afternoon thunderstorms, this land-sea breeze transition is facilitated by the onset of thunderstorms and their resulting cold pools (Chen et al., 2014). Chen et al. (2014) also found that when there is a thunderstorm, the land breeze persists from the afternoon of the thunderstorm day until the next morning, sweeping out polluted air. This means that it is also important to understand land-sea breeze circulations to understand the effect that thunderstorms have on ventilation mechanisms.

1.2 Urbanization

As urban areas expand, they develop unique features that separate them from their surroundings. Some of these features include man-made structures, concrete and asphalt surfaces, and less greenery. The existence of these features can have an effect on local

meteorology through something known as the Urban Heat Island (UHI) effect. According to the Environmental Protection Agency (EPA), these heat islands "are urbanized areas that experience higher temperatures than outlying areas." This increase in temperatures is due to the material with which cities are constructed. Concrete and asphalt, for example, have large thermal inertia and can store large amounts of heat (Han et al., 2014). The absorbed heat is then re-emitted into its surrounding environment, creating a heating effect. Due to the concentrated nature of cities and the lack of green spaces (parks, forests, marshes, lakes, etc.), the absorbed and re-emitted heat creates a concentrated "island" of high temperature areas. In comparison, nearby regions with more natural landscapes, like forests or lakes, have a daytime temperature of about 0.5 – 3.9ºC lower on average than an urban area and a nighttime temperature of about 1.1 – 2.7ºC lower on average (EPA, 2021). These UHI characteristics impact the mesoscale circulation and therefore affect weather patterns in the vicinity, including the behavior of thunderstorms.

Research on the effects of urbanization on thunderstorms has roots in the La Ponte anomaly which found that there was an apparent enhancement of precipitation downwind of Chicago (Changnon, 1968), followed by the Metropolitan Meteorological Experiment (METROMEX, 1971-1975) in the St. Louis area (Changnon et al., 1977; Ackerman et al., 1978). They found increased cloudiness, total rainfall, and severe storm activity downwind of St. Louis in the summer. Atmospheric stability studied by Baik et al. (2007) found that the UHI-induced circulation can become strong in a nearly neutral or less stable boundary layer in the daytime, suggesting that this is the cause of late afternoon or evening thunderstorms in urban settings. Craig and Bornstein (2002) did a modeling simulation with and without the city of Atlanta. They found that the city's presence created a region of confluence leading to convergence and upward motion, and therefore linking UHI to precipitation initiation. Similarly, Lin, C., et al. (2011) did

a modeling study of the impact of UHI on precipitation over complex terrain and found that there is enhanced rainfall downwind of Taipei and upwind plain areas.

Taipei has grown and urbanized since the 1960s into an important trade center in both East and Southeast Asia (Chen et al., 2007). As with any other city that becomes a major economic and political center, there is an increase in urbanization that comes with population growth and changes in land use. In that time, the changes in albedo, surface roughness, and sensible heat appear to have impacted the formation and characteristics of afternoon thunderstorms. Shepherd et al. (2002) found that the increase in precipitation downwind was due to higher temperatures in the city compared to the surrounding areas creating increased instability and convective activities. Alongside the increased instability, the increased surface roughness favors surface converge, as Craig and Bornstein (2002) found with Atlanta. Lin et al. (2008b) studied the UHI effect in Taipei and found that the excess heating not only affects land-sea breeze circulation but also that the proposed 1.5ºC increase in temperature due to urbanization found by Chen et al. (2007) could be as high as 4º–6ºC. Chen et al. (2007) also attributed an increase of more than 67% in the frequency of afternoon thunderstorms and an increase of 77% in the rainfall generated to urbanization. Lin, C., et al. (2011) used satellite data to model the impact of urbanization coupled with the orography of the Taipei Basin, as previously mentioned, to better understand the results Chen et al. (2007) and other studies had. They found that the urban area of Taipei can delay precipitation initiation by acting as a warm and dry center that stops the sea breeze from reaching the mountains where convection generally begins. However, the sensible heat flux present allowed the air masses to become more unstable and produce heavy convection. Kuo and Wu (2019) further built on these studies to find a more direct relationship between UHI and precipitation over the Taipei Basin. Through model

simulations, they were able to find that in the presence of UHI, sea breeze convergence is enhanced in the southern part of the basin, enhancing convection. In the absence of UHI, convection is delayed due to lower wind speeds and weaker convergence resulting in weaker surface precipitation.

1.3 PM2.5

An increase in aerosol emissions and air pollution goes hand in hand with urbanization. Aerosols, including PM2.5, can affect weather patterns by acting as cloud condensation nuclei (CCN) and affecting the development of clouds and precipitation. While PM10 and PM2.5 are usually studied together, this study focused on PM2.5 due to the similarity it has to fine aerosols that act as CCN for rain nuclei, rather than PM10, which contains coarser aerosols that generally work as ice nuclei. Generally, when the number of aerosols increases, the number of CCN increase, causing the average droplet size to decrease, potentially suppressing precipitation. However, some studies show that under the right conditions, precipitation is actually enhanced. Han et al. (2012) used a two-dimensional cloud model to examine how increased aerosol concentration in urban areas affects precipitation induced by urban heat islands. The authors found that strong convective clouds develop in a high aerosol environment because of increased latent heat from enhanced condensation. A large liquid water content (LWC) can also be found at higher levels increasing riming and producing large ice particles, which enhances melting and precipitation downwind of the urban area. In addition, Rosenfeld et al. (2008) discussed how when aerosols act as CCN, they can change the storm cloud composition by delaying the conversion of cloud drops into rain or precipitating drops. A delay in conversion leads to a delayed rain start time and a larger rainfall total.

Similarly, Alizadeh-Choobari (2018) used modeling simulations to look at the effect of aerosol concentrations on precipitation over different terrains. The authors found that the onset of precipitation is delayed in a polluted environment. However, the overall precipitation rate and total amount are higher, especially over a flat land region south of a mountainous region. Heavy and moderate precipitation increased more in a polluted environment than light precipitation, which the authors attributed to differences in relative humidity. When there is an ample amount of water vapor, precipitation totals increase. However, insufficient water vapor leads to particulates competing to collect water vapor, increasing the number of small droplets but decreasing the total precipitation. The authors concluded that "an increase in the aerosol number concentration inhibits light warm rain processes, but fosters intense ice precipitation processes" (Alizadeh-Choobari, 2018).

Understanding the impacts of aerosols on precipitation prompts the question, what are the aerosol trends over Taipei like? Hsu and Cheng (2019) looked at PM10 and PM2.5 through a cluster analysis of daily averaged wind fields and sea level pressure from surface stations in Taiwan from 2013 to 2018 to identify the synoptic weather patterns and the corresponding air pollutants. Their study found that clusters that corresponded to the warm seasons (May- October) had the lowest PM concentrations, which was attributed to the warm season also being the rainy season in northern Taiwan and therefore having a lot of washout. This paper concludes that the relative concentrations in summer months may not have a broad range due to regular washout, in comparison to other seasons where large amounts of aerosols are advected into the region. However, after a convective event, we can expect the concentration of aerosols measured to decrease, perhaps even below the mean concentration.

There are extensive studies about summer afternoon thunderstorms over the Taipei Basin, their changes over time, and the impact that urbanization has had on them. However, there is a lack of research on the impact aerosols may have on thunderstorms over the Taipei Basin, especially in regard to extreme events. It is of great significance to understand how aerosol trends have progressed over the Taipei Basin as the city continues to grow and expand and if that has contributed to the severity of thunderstorm events, since an increase in extreme events would pose a higher risk to the infrastructural development of the city. The goals of the present study are:

1. To better understand the behavior of PM2.5 in the summer months from 2005 to 2015, both spatially and temporally, while taking into consideration the difference between days with high versus low PM2.5 concentrations.
2. To analyze heavy precipitation events by looking at rainfall characteristics alongside PM2.5 concentrations to see if there is a relationship between the diurnal cycle of both.
3. To understand the impact of low versus high PM2.5 concentrations on heavy precipitation events.

Section 2 provides a summary of the data used and the methods of analysis. Section 3 looks into the PM2.5 concentrations over the Taipei Basin from different angles. Section 4 analyzes three different case studies to see their key characteristics and how these vary between events. Section 5 uses the Weather Research and Forecasting (WRF) model to understand the impact of PM2.5 concentrations on heavy precipitation events. Section 6 discusses the results and key findings.

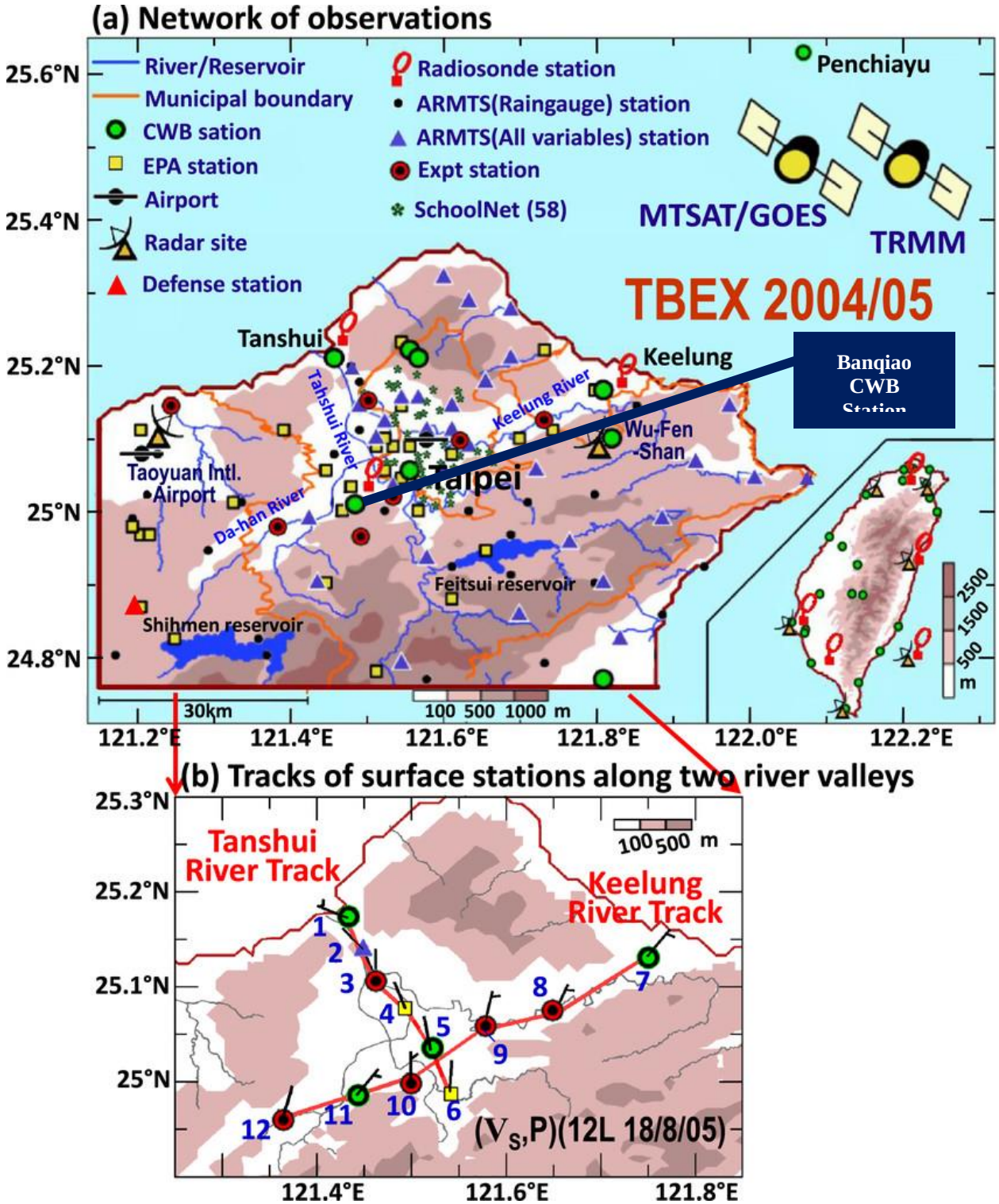

Figure 1 Adapted from from Chen et al., 2014 Figure 2 showing the stations used for experiment. For reference, Banqiao has been highlighted using a navy insert box. ***© American Meteorological Society. Used with permission.***

2 Data and Methods

The present study had four main phases: classifying weak synoptic events, analyzing PM2.5 data, analyzing rainfall data, and running a WRF experiment. The details on the data used and the methods is below.

2.1 *Classifying Weak Synoptic Events*

To find the precipitation events whose accumulation amounts were solely due to local triggers, as afternoon thunderstorms are, only weak synoptic events were used in the data analysis. It is essential to analyze only the weak synoptic events because a weak synoptic environment means that the impact of horizontal advection of particulates is reduced so that there is a constant background mean. A weak pressure gradient from a weak synoptic environment also limits the variability that horizontal advection can add. Weak synoptic events would be expected to have minimal particulates from outside sources; instead, local sources will be the main contributors to the Taipei Basin's PM2.5 concentration.

Filtering for weak synoptic events was done using Japan Meteorological Society (JMS) surface weather maps and NOAA GIBBS satellite images to find the location and extent of fronts and tropical cyclones. Only 55 days met the top 5% rain criteria and were classified as weak synoptic events. Mean synoptic conditions of the 55 days were analyzed to create a composite map (Figure 2). The map shows weak gradients in the pressure field. The isobars dip along southeast China, forming a local trough extending up to the south of the Korean peninsula, indicating a stationary front to the northeast of Taiwan. This feature is also often present in surface weather maps.

2.2 PM2.5 Data

PM2.5 data were analyzed using data from 18 Taiwan Environmental Protection Agency (EPA) stations over the Taipei Basin (Figure 3, Table 1). Data was consistently recorded and reported starting in 2005, so only the data from 2005 to 2015 over the Taipei Basin (defined as 25.1095±0.2, 121.4697±0.2) during the summer months (June, July, August).

The hourly concentration at each station was used to calculate various means to compare changes in PM2.5 concentrations at specific times and points. The summer mean was calculated using all of the hourly concentrations from all the stations and averaging them for each year from 2005 to 2015. Further, the hourly average at each station was also calculated by taking the hourly concentration at each station during heavy rain (HR) events and averaging the values from 2005 to 2015.

2.3 Rain Data and Methods

Observation datasets were used to study the afternoon thunderstorms in the Taipei Basin and determine the days that could be used for analysis. Only extreme events categorized as the top 5% of all precipitation events are studied to ensure that the analyzed rainfall events reach the heavy rainfall characteristic of a summer afternoon thunderstorm. The extreme event threshold was selected using the Taiwan Climate Change Projection and Information Platform (TCCIP, https://tccip.ncdr.nat.gov.tw/) project dataset 1 km x 1 km gridded daily precipitation over all of Taiwan from 1960 to the present day. In this study, only the data from 2005 to 2015 was used over the Taipei Basin (defined as 25.1095°±0.2°, 121.4697°±0.2°) during the summer months of June, July, and August.

Extreme events were initially classified as the top 1% of rainfall-producing storms, but the threshold for an extreme event was changed to the top 5% due to the limited sample number.

All of the daily rainfall totals for June, July, and August of 2005-2015 were sorted, and it was found that the top 5% rainfall totals needed to be at least 81.24 mm/day. For this reason, only the events with 81.24 mm/day or more were considered the top 5% and used for further analysis.

Hourly rainfall data from Taiwan Central Weather Bureau (CWB) automated surface stations (Automatic Rainfall and Meteorological Telemetry System ARMTS) (Figure 4, Table 2) was used to analyze the spatial and temporal extent of the heavy rain events. The CWB standards for heavy precipitation and flood risk events (https://www.cwb.gov.tw/V8/E/P/Warning/W26.html) were used to analyze the severity of the heavy rain events, by highlighting stations that met the criteria to be classified as a potential hazard. A single-day event and a three-day event (three consecutive days with heavy rain) were selected to analyze further and compare the diurnal cycles of PM2.5 to the heavy rain. The temporal and spatial distribution of rainfall during a Mei-Yu event was also analyzed to benchmark what strong synoptic rainfall events are like. The data from the Mei-Yu case was only used to compare to the other case studies presented. The data was not used in any other averaging or statistical measurement unless explicitly stated.

2.4 Testing Microphysics Sensitivity of Precipitation to Varied PM2.5 Concentrations Using WRF

In order to test the sensitivity of rainfall to different aerosol concentrations, several experiments were conducted using the National Taiwan University two-moment microphysics scheme (Cheng et al. 2007, 2010). This NTU scheme allows for the modification of the microphysical development of storm clouds and the selection of different concentrations of aerosols in the atmosphere. Three concentrations (continental clean, continental average, continental polluted) were selected to represent three different PM2.5 concentrations during storm development (*clean, average, polluted*). The three concentrations have an

aerosol distribution based on Cheng et al. (2007, 2010) and Rosenfeld et al. (2008), where aerosols were classified into different types, including clean, average, and polluted. These are representative categories and do not have specific size distributions over Taipei, but the general concentration totals reflect general continental clean, average, and polluted conditions.

Of the 55 days analyzed in the PM2.5 section, July 5, 2007, a case with high PM2.5 concentration was selected as a representative case due to its synoptic similarity to the mean composite. The case was simulated using the National Taiwan University two-moment version of the WRF-ARW (v.3.8.1) model. A triply nested simulation with the respective grid size of 12, 4, and 1.33 km used the synoptic environment over East Asia to set up the conditions in which most of the event days occurred. The outermost domain (D01) is focused over East Asia and covers an area of 2221 km x 2460 km, the second domain (D02) is focused over the greater Taiwan region and covers an area of 703 km x 1110 km, and the innermost domain (D03) is focused directly over the island of Taiwan itself and covers an area of 377 km x 176 km. The model physics schemes across all three domains include the following: the New Teidtke Scheme was used for cumulus parameterization (Zhang et al., 2017), the Yonsei University PBL scheme (Hong et al., 2006), the New Goddard Shortwave and Longwave scheme (Chou et al., 1999, 2001), and the Unified Noah Land Surface scheme (Tewari et al., 2004).

All three domains were integrated for 30 hours starting at 1800 UTC July 4, 2007 with hourly outputs. The initial conditions were interpolated from National Centers for Environmental Information (NCEI) Global Forecast System (GFS) 1º analysis data at 6-hour intervals. The model was integrated three times, each with a different aerosol concentration (*clean, average, polluted*), and the resulting rainfall patterns and totals were compared.

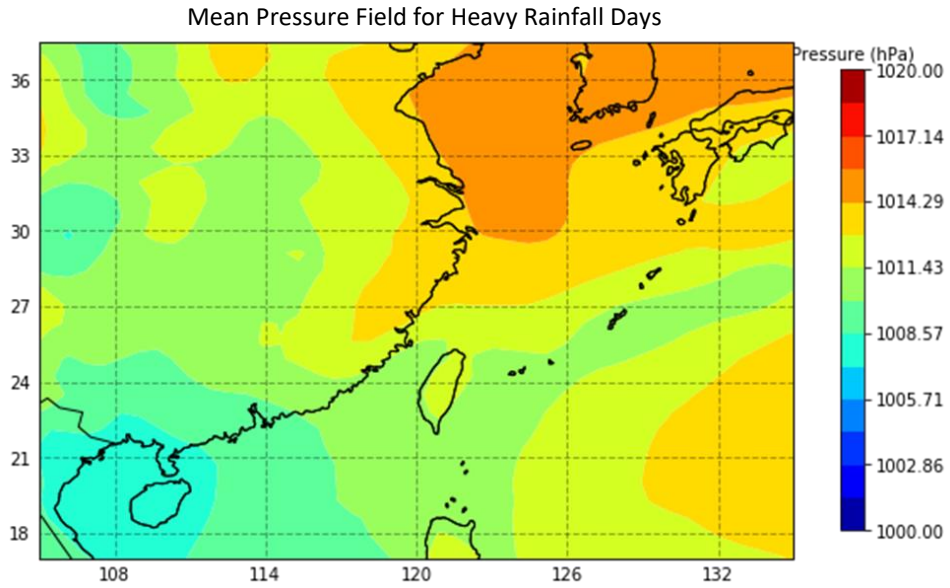

Figure 2: Surface pressure composite of the 55 heavy rainfall days over East Asia.

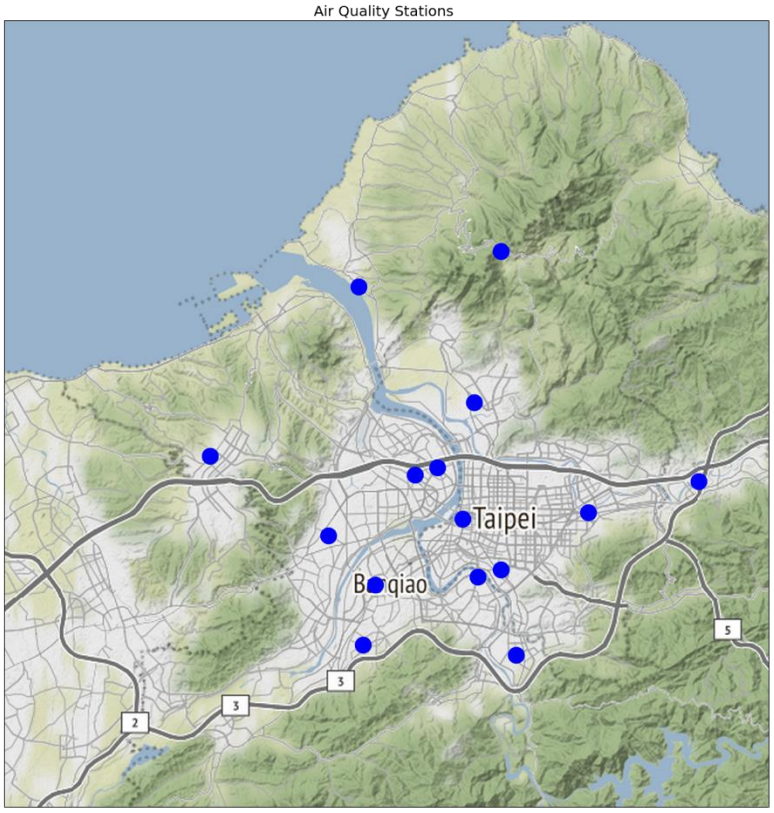

Figure 3: Map of the Taipei Basin with the air quality stations marked by blue dots.

Table 1: Air quality stations (Chinese name, English name, latitude, longitude)

Chinese Name	English Name	Latitude	Longitude
汐止	Xizhi	25.065669	121.6408
萬里	Wanli	25.179667	121.689881
新店	Xindian	24.977222	121.537778
土城	Tucheng	24.982528	121.451861
板橋	Banqiao	25.012972	121.458667
新莊	Xinzhuang	25.037972	121.4325
菜寮	Cailiao	25.06895	121.481028
林口	Linkou	25.07857	121.365703
淡水	Tamsui	25.1645	121.449239
士林	Shilin	25.105917	121.5145
中山	Zhongshan	25.062361	121.526528
萬華	Wanhua	25.046503	121.507972
古亭	Guting	25.020608	121.529556
松山	Songshan	25.05	121.578611
大同	Datong	25.0632	121.513311
陽明	Yangming	25.182722	121.529583
三重	Sanchong	25.072611	121.493806
永和	Yonghe	25.017	121.516306

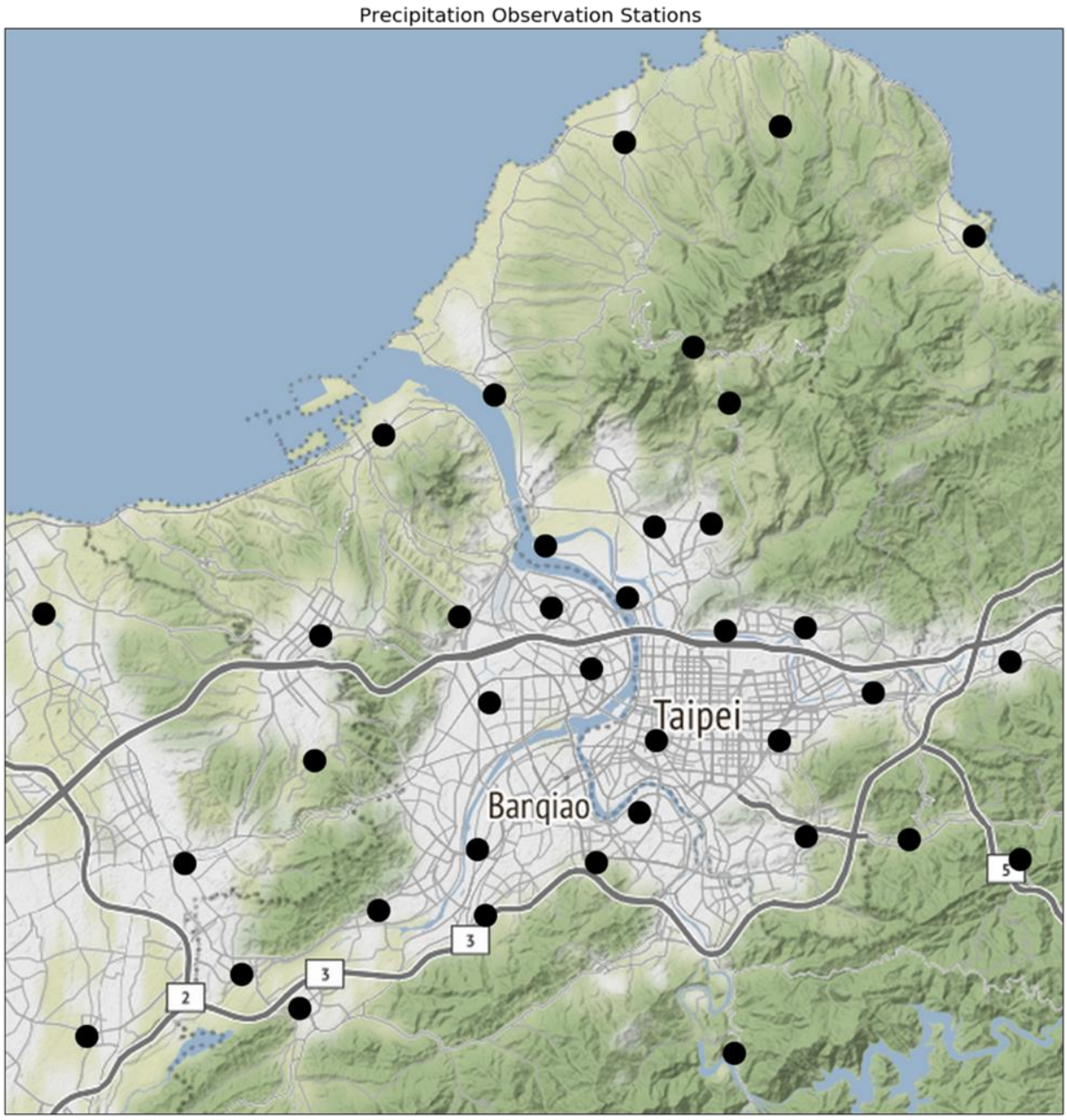

Figure 4: Map of the Taipei Basin with the precipitation stations marked by black dots.

Table 2: Precipitation stations (name, latitude, longitude)

Station ID	Latitude	Longitude
C0A52	24.98	121.39
C0A58	24.92	121.54
C0A64	25	121.65
C0A68	25.09	121.43
C0A71	25.08	121.37
C0A92	25.27	121.56
C0A94	25.23	121.64
C0A98	25.11	121.46
C0A9A	25.08	121.53
C0A9B	25.12	121.51
C0A9C	25.12	121.53
C0A9E	25.09	121.49
C0A9F	25.08	121.57
C0A9G	25.06	121.59
C0A9I	25.06	121.48
C0AC6	24.94	121.36
C0AC7	25.04	121.56
C0AC8	25	121.57
C0ACA	25.05	121.44
C0AD0	25.26	121.49
C0AD1	25.15	121.4
C0AD2	25	121.61
C0AD3	25.09	121.46
C0AD4	24.97	121.44
C0AD5	24.95	121.34
C0AG9	24.99	121.48
C0AH0	25.07	121.65
C0AH1	25.01	121.5
C0C48	24.99	121.32
C0C49	24.93	121.28
C0C62	25.09	121.26
C0C64	25.03	121.37

3 PM 2.5 Analysis

A detailed analysis of PM2.5 in the Taipei Basin from 2005 to 2015 is included here to provide insight into the particulate trends given continual urban development and increased environmental awareness, the background state that heavy rainfall events are occurring in, and the effects of rainfall on particulate concentrations.

3.1 Temporal Analysis

A temporal analysis of PM2.5 concentrations paints a picture of how concentrations may vary during different times of the day and year by year (2005-2015). Specifically, an analysis of PM2.5 concentrations over the Taipei Basin during the summer months of June, July, and August (JJA) is essential to understand what the general background state of the particulates is and if continuous urbanization or increased environmental awareness has affected the average concentration. Without filtering for weather patterns, the ten-year summer (JJA) average diurnal cycle along with the summer mean for each of the ten years is presented in Figure 5. A ten-year summer average is important because it serves as a control or constant variable for any other studies or calculations done about changes in PM2.5 throughout the decade. The ten-year average is a background state in which HR events occur and serves as a guide for how much different PM2.5 concentrations deviate.

In Figure 5, there appears to be a decreasing trend throughout the years, with the first few years having higher concentrations than the later years. While there may be some mesoscale factors that play into the yearly averages, like an abnormally active typhoon season (as is the case for August 2015) or above-average Mei-Yu rainfall, the change in mean concentration was attributed to a policy passed by the Taiwan EPA in 2012 limiting the 24-hour value and the

yearly average of suspended particulates in air quality standards (https://airtw.epa.gov.tw/ENG/Information/Standard/Rules.aspx).

It is also noteworthy that the diurnal cycle in all of the years exhibits a sort of double peak in PM2.5 concentrations. There is a continuous increase from about 11–14 Local Standard Time (LST), reaching a peak around 12 LST followed by a slow decline in the concentrations. The peaks can be attributed to the emissions from the morning rush hour with people going to work and school, building up over time and concentrating as the atmosphere becomes more stable during the day. From the observation cases and previous research like Alizadeh-Choobari (2018), it is inferred that during the summer, there is rainfall that causes washout and/or the atmosphere begins to mix. The particulates that had concentrated close to the surface begin to get mixed out and the concentration at the measurement stations decreases. From 19–21 LST, the concentration of PM2.5 increases again, which is unexpected but can be due to a second rush hour as people go home from work, school, and cram or after-school study schools. Large emissions of particulates over a long period once again allow for an accumulation near the surface where the measuring stations are until the atmosphere mixes out the particulates and advects them away.

3.2 Spatial Analysis

Studying the spatial distribution of PM2.5 is crucial because it can give insight into which areas in the basin have higher concentrations than others and perhaps where most emissions are concentrated. The hourly PM2.5 concentration for each of the 55 HR days was averaged for each station over the Taipei Basin to analyze the spatial distribution of PM2.5. The diurnal cycle for each station makes it easier to pinpoint which locations have a higher concentration and then identify them on a map. Figure 6 shows the diurnal cycle of each station in the basin, and three stations stand out: Sanchong and Zhongshan have the highest concentrations on average, while

Yangming has the lowest concentration (locations shown in Figure 7). Upon further analysis, it is determined that the Sanchong and Zhongshan stations are located close to major highways and are also in the city's center. In contrast, Yangming is situated at a higher elevation and further away from the highly urbanized center. This shows that stations located close to high emission areas like highways will have higher PM2.5 concentrations than stations located further away from urban centers.

Isolating the information for each station allows for multiple types of analysis and finding new clues to the PM2.5 patterns in Taipei. Similar to Figure 5, Figure 6 also displays noticeable peaks in the stations' average diurnal cycle. The first peak occurs at the same time as the yearly JJA diurnal cycle, around noon, and is well defined at all of the stations. However, it is interesting to note the evening/ second peak in the station averages because these station averages are for days with heavy rainfall in the afternoon. This means that local sources emit enough particulates to increase the PM2.5 concentration despite heavy rain and washout of particulates. Unlike the first peak at noon, the second peak is not present or well defined at all stations, including Xindian, Songshan, and Yangming. These three stations are all located along the outer perimeter of the city center and possibly further away from the largest evening emission sources.

3.3 Comparative Analysis of PM2.5 Concentrations Using Temporal and Spatial Markers

Understanding the general spatial distribution and temporal changes throughout the past decade provides a general background picture, but breaking down the data by stations, time, and concentration is imperative to fully understand the PM2.5 trends of heavy rain events. Data analysis from different angles provides a more comprehensive view of the response of particulates to rainfall.

3.3.1 Temporal Mean Analysis

In order to see if there is even anything special about the PM2.5 concentration on HR days, the easiest thing is to compare the diurnal cycles of HR days to summer days in the same years without any precipitation. Non- convective or non-rainfall days aren't considered weak synoptic days since they generally have a low-pressure system, such as a tropical cyclone in the vicinity forcing a more stable environment and subsidence trapping the particulates over the northern part of Taiwan in the Taipei Basin. Without any rain to wash out the particulates or advection to mix the air and move the particulates out, the constant output of particulates allows the concentration to remain stable and not decrease throughout the day so that, on average, they are 5μg/m3 higher concentration than that of days with heavy rain (Figure 8).

Besides just comparing the PM2.5 concentrations of HR days to days without rainfall, HR day concentrations can also be compared to the background summer mean since it is a constant. The summer mean gives a point of comparison for how the other two diurnal cycles vary from their background environment. It makes sense that HR days would have a lower concentration of particulates than the summer mean because there is rainfall occurring on these days. The summer mean consists of days that have HR, tropical cyclone, and Mei-Yu rainfall events. The large-scale flow can at times be conducive for particulate washout and strong ventilation, removing particulates from the atmosphere and reducing overall measurements. This, in comparison to the synoptic state of non-HR days, is very different as there is no chance for washout, and there is generally strong subsidence causing the particulates to be trapped, thereby increasing the overall concentrations.

To better understand what kind of environment heavy rainfall events were happening in, the mean diurnal cycle of the days before (PRE) and after (POST) heavy rain (HR) events was

calculated only using the isolated HR events (Figure 9). Here, isolated means that if there was an HR event the day before or after, those days were not taken into account for averaging. Comparing the diurnal cycles of PM2.5 for three days (PRE, HR, POST) gives a better picture of the background state in which the storms are occurring and how rain affects the accumulation patterns and the recovery rate after washout. The diurnal cycle for PRE is lower than that of days with no rain, implying that even though there may be no precipitation, the environment is different, and that is reflected in the PM2.5 concentrations. PRE and HR days also seem to parallel each other until rainfall, and the particulate concentration decreases significantly on HR days. This is further reflected in POST's initial concentration (15.11 μg/m3) as it is much lower than the initial concentrations of PRE (19.34 μg/m3) and HR days (18.11 μg/m3). However, as the day progresses, the concentration of POST surpasses the concentration of HR days at 12 LST (25.44 μg/m3), and continues to rise so that by the end of the day it has even passed the concentration of PRE (19.14 μg/m3). The ending concentration of POST (19.54 μg/m3) is still lower than the ending concentration of a non-rainfall day by about 3 μg/m3, meaning that with two consecutive days of no rain, given the recovery rate of particulate emission and the constant emission rate of the local sources, the diurnal cycle values would possibly be similar to those of the non-rainfall days.

PRE and POST concentrations were calculated to paint a full three-day picture of PM2.5 concentrations before, during, and after a heavy rain event. To better visualize the concentration trends, the same PRE, HR day, and POST concentrations are put in consecutive order to give a picture of the timeline of the PM2.5 concentration while also comparing it to the background summer mean. Figure 10 (top) shows the averages as a consecutive three-day sequence with rainfall and night/day colorings. The average diurnal cycle of the three days (blue) coincides

with the background summer mean (green) on the PRE section and begins to deviate when precipitation begins, with the average diurnal cycle having lower values than those of the summer mean. Besides the difference caused by washout, there is not much difference between the average and summer mean. Figure 9 (bottom) shows the difference between the average and summer mean (yellow), and once again, the biggest difference occurs when there is precipitation. The key points of this figure are the differences between the three-day diurnal cycle and the summer mean. Initially, there is not much difference (during PRE), but once it begins to precipitate there is a large difference as the HR day concentration decreases. Afterwards, there is a sharp increase during POST, marking the recovery of the particulate concentration. Despite various changes in the concentration of the three-day sequence, the amount that it can have values higher than the summer mean are negligible.

3.3.2 PM2.5 Concentration Quartiles

Another way that the PM2.5 concentrations for the 55 HR days can be analyzed is by breaking down the concentrations into quartiles from highest to lowest. Quartiles based on PM2.5 concentration allow for isolation of the conditions in which various concentrations occurred and how each type of concentration responds to precipitation. The (13) days that have the highest PM2.5 concentration on average were called DIRTY, the (13) days with the lowest PM2.5 concentration were called CLEAN, and the remainder of the days were grouped as OTHER days. As a reminder, the temporal analysis indicated that the average yearly concentration decreased from 2005 to 2015. The majority of days in the DIRTY quartile are from before 2010, and most days in the CLEAN quartile are from 2012 after. Figure 11 shows the diurnal cycles for each quartile, and it is interesting to note that OTHER and DIRTY have the double peak seen in the other diurnal cycles, but CLEAN does not. The fact that CLEAN only

has a peak in the middle of the day may imply a strong response to the rainfall that occurs in the afternoon. Regardless of the continuous emissions in the afternoon and evening, the PM2.5 concentration can never recover to peak a second time in the evening.

To further investigate the differences between the diurnal cycles of CLEAN, OTHER, and DIRTY, the ten-year summer mean (found in Figure 5) and the HR day average (found in Figure 6) were compared in Figure 12 by placing them all on the same graph. The similarity between the summer mean, HR day average, and OTHER is worth further study. The diurnal cycle of the HR days that are not at either end of the PM2.5 concentration spectrum mirrors the background PM2.5 state in which they occur. Since there is a difference between the summer mean and CLEAN and DIRTY, the easiest way to compare the actual differences is by subtracting the summer mean from the quartile diurnal cycles (Figure 12, right). The first thing that can be noted is how the difference between the OTHER days and the summer mean is more or less zero throughout the whole 24-hour period. CLEAN days have the largest negative difference, which makes sense because the average concentration on these days is less than the other days, hence the name CLEAN. Similarly, the DIRTY days have a positive difference, though not as large as the difference between CLEAN and the HR day/ summer mean. All three quartiles have a similar trend in differences through the middle of the day (9 LST to 14 LST), as seen in Figure 12, right. However, when the afternoon/evening rush hour peak in PM2.5 concentration occurs, there is a difference in response to precipitation. The summer mean, used as a constant, averages across various weather conditions. This means that the summer mean trend includes PM2.5 responses to strong synoptic events, high pressure systems, heavy rainfall events, etc. For this reason, the response to afternoon rainfall is bound to be less explicit than OTHER and CLEAN, which are only affected by heavy rainfall events. However, contrary to the initial hypothesis that washout

would be the greatest on days with a high PM2.5 concentration, there seems to be no difference when heavy precipitation occurs, possibly implying that DIRTY days do not respond to precipitation washout.

A closer look at the PM2.5 concentration and rainfall totals of CLEAN and DIRTY provides a clearer picture of the differences that both quartiles have in response to precipitation. Figure 13 breaks down the measurements for each of the days in the CLEAN and DIRTY quartiles to see if there are differences in the rainfall times and totals compared to the decreases in particulate concentration. CLEAN days are analyzed in the top row and DIRTY days on the bottom row. The PM2.5 concentration is on the left, and the rainfall is on the right. The light blue line and the dark blue line represent the day with the lowest particulate concentration (August 27, 2015) and the day with the highest particulate concentration (June 16, 2008) in CLEAN, respectively. Both days start similarly, but once the rainfall occurs, June 16, 2008, increases in particulate concentration, unlike the rest of the days in the quartile. The brown and tan lines represent the day with the lowest particulate concentrations (June 21, 2010) and the day with the highest particulate concentrations (July 7, 2005) in DIRTY, respectively. Just like the day with the highest concentration in CLEAN, the day with the highest concentration in DIRTY also increased in concentration after rainfall occurred. An increase in PM2.5 concentration despite a heavy rainfall event means that the rate at which PM2.5 particulates are being emitted is higher than the rate at which rainfall can wash them out. The reason for the increase in concentration in these particular cases is unknown and may present a future research topic. Despite these differences between all the cases in both quartiles, the averages still represent the diurnal cycle on the majority of HR days.

In Figure 13, the precipitation averages for each quartile are shown to be a middle ground for the rainfall totals for each set of days due to the large range of values. Even though a couple of the days in CLEAN reached or exceeded 300 mm at a given hour, the maximum average hourly total is less than 200 mm. In contrast, only two days exceeded 300 mm at a given hour, and the maximum average hourly total is about 100 mm. This difference in maximum average rainfall is the first clue that perhaps it rains less when there is a high concentration of particulates. Since there is an extensive range in the rainfall amounts per day, a relative total accumulation was calculated by adding all of the rainfall in each quartile and dividing it by the number of days. This way, the large range in totals is consolidated into a single rainfall total for each quartile. The relative accumulation total for a day in CLEAN is 344.73 mm, while the relative total for a day in DIRTY is 328.71 mm meaning that there is only a difference of 20 mm/day. While the difference is not large, it supports the previous finding that there is less rainfall when the concentration of particulates is high.

The extremes of CLEAN and DIRTY were compared to see if the differences in response to rainfall could be attributed to a difference in the rainfall pattern of the days. Figure 14 shows the PM2.5 concentration and precipitation for August 27, 2015 (lowest concentration, CLEAN), June 16, 2008 (highest concentration, CLEAN), June 21, 2010 (lowest concentration, DIRTY), and July 7, 2005 (highest concentration, DIRTY). From the previous analysis in Figure 13, it was noted that both of the lowest concentration days in CLEAN and DIRTY had the PM2.5 concentration decrease after rainfall, while the highest concentration days had the PM2.5 concentration increase despite rainfall. Figure 14 highlights this by having the PM2.5 concentration overlayed with the rainfall. The lowest concentration days reach their peak around 12 LST, and then once the rain begins, there is a marked decline in the average concentration.

June 16, 2008 has an early peak around 10 LST, and then there is a slight dip in the measurements as the precipitation starts. Still, then as the precipitation gets heavier, the PM2.5 concentration continues to increase, even after the rain has stopped. July 7, 2005 is different because there is no peak, but rather the particulate concentration increases throughout the day and increases significantly more once the rain begins to fall.

3.3.3 Spatial Analysis

Rainfall station data was used to analyze the rainfall trends to see if perhaps rainfall amounts vary significantly between the four days. Figure 15 shows the number of hours that precipitation was recorded at each station and the precipitation totals for each of the four days. Only the fifteen stations that existed in 2005 were used for analysis to prevent errors that could be introduced by having a different number of stations recording data each day. Notably, the CLEAN days have significantly longer average rainfall times per station than the DIRTY days. Still, the difference is not as significant when comparing the lowest concentration and highest concentration days. For reference, August 27 (lowest concentration, CLEAN) and June 21 (lowest concentration, DIRTY) recorded precipitation for an average of 10.94 and 3.31 hours, respectively. There is a large difference in the rainfall duration and the rainfall totals, which does not support the hypothesis that the lower concentration days would precipitate for a more extended period. In addition, high concentration days do not precipitate for a significantly shorter period than their low concentration counterparts; June 16 averages 7 hours of rain, and July 7 averages 2.2 hours of rain.

Since there was no clear signal from the duration and rainfall totals of the extremes in DIRTY and CLEAN, the spatial distribution of rainfall and PM2.5 concentration was analyzed to see if they could explain why there is such a difference in the PM2.5 response to rainfall. If

precipitation is limited to a small area on the high concentration days and not across the whole basin, then perhaps that would explain why the PM2.5 concentration did not decrease. For this reason, Figure 16 shows rain and PM2.5 observation stations. Stations recording precipitation are denoted with a blue circle, and the size of the circle corresponds to the precipitation amount. Any stations that did not record precipitation are denoted with a black circle. The air quality stations are indicated with a diamond shape, and the colors reference the concentration at the location. Figure 16 shows precipitation recorded at stations across the basin and not limited to a specific region on any of the four days. In addition, there was precipitation recorded at stations that are in the vicinity of PM2.5 observation stations. The key point being that the amount of precipitation recorded at each station marks a bigger difference than the spatial extent of the rainfall. This lack of difference in spatial extent counters the previous hypothesis that precipitation on high concentration days would be more localized and not reduce particulate concentrations enough to bring down the average diurnal cycle.

A composite of the synoptic conditions for CLEAN and DIRTY days was created to look for more clues as to why there were different responses to rainfall. Using JMS surface weather maps, the most defining feature of CLEAN is a front to the north over southeast China extending to southern Japan, similar to the synoptic composite of the 55 HR events. Figure 17 shows the mean synoptic conditions for CLEAN as a pressure gradient with a high to the east and a low to the west of Taiwan. The strong pressure gradient may allow for some winds, albeit weak, to impact the flow over northern Taiwan and therefore allow for basin ventilation, decreasing the concentration of PM2.5 particulates. The synoptic conditions for DIRTY have a comparably weaker pressure gradient, with the main defining features being a high-pressure system to the east and a low to the west. A weaker pressure gradient means that there are likely no pressure-

induced winds that will affect the airflow over the basin allowing for the local sources to saturate the air, leading to higher concentrations.

3.4 Summary

There are various differences in the PM2.5 concentration in the Taipei Basin from 2005–2015. Some of these differences are due to policy changes and varying weather patterns, but different signals come up even when focusing on extreme precipitation events. Most notably, some events have the PM2.5 concentrations responding actively to precipitation, while in other cases, the concentration is not affected or even increases, according to observations. On average, the particulate concentration on HR days does not vary significantly from the background summer mean; different PM2.5 concentrations have different responses to precipitation.

A summary of the key take aways from this chapter are:

1. The annual average of PM2.5 decreased in general from 2005–2015
2. The spatial distribution of PM2.5 concentrations was linked to the location of the station. Stations close to the center of the city where there is significant traffic and industrial activity had the highest PM2.5 concentrations, while stations more in the outskirts of the city near the mountains had the lowest concentrations.
3. When comparing PM2.5 mean concentration of the HR days to non-HR days (days with no rainfall) their diurnal cycles followed similar trends, but HR days had consistently higher concentrations
4. If the diurnal cycles of the HR day PM2.5 mean is compared to the PM2.5 concentration of the days before (PRE) and the days after (POST), the expected trend of lower PM2.5 concentrations after rainfall is observed. However, at the end of the POST day, the PM2.5

concentration is higher than at the beginning of PRE, speaking to the recovery rate of PM2.5.

5. When comparing the composite diurnal cycle of PRE, HR days, and POST to the summer background mean, it is notable that there is not much difference between the composite diurnal cycle and the summer mean. The only time there is a significant difference is immediately after rainfall when the HR day concentration drops 5 µg/m3 compared to the summer mean.
6. When the PM2.5 concentration of HR days is separated into quartiles (based on concentration) it seems like DIRTY days do not respond to precipitation (don't show washout characteristics). This is further exemplified in Figure 14 where the concentration actually increases after rainfall.

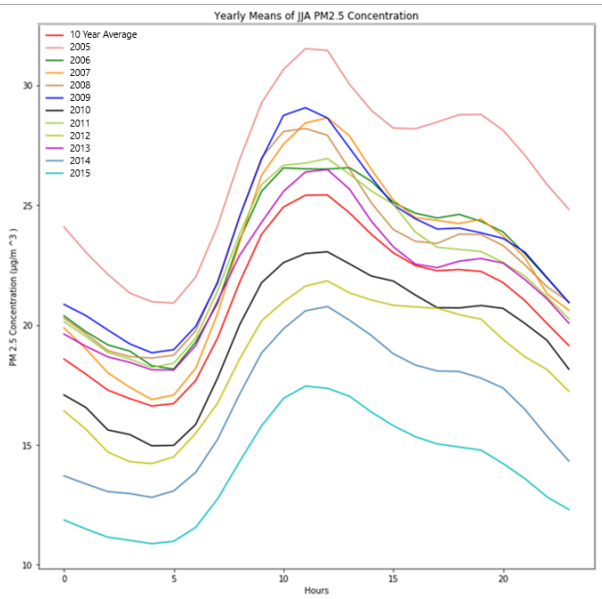

$PM_{2.5}$	24 hours value	35	µg / m^3
	Yearly average	15	

Source: EPA

Figure 5: Yearly means of PM2.5 of the summers (June, July, and August) from 2005 to 2010. The bottom table is an excerpt from the Taiwan EPA order on May 14, 2012 about the new PM2.5 regulations.

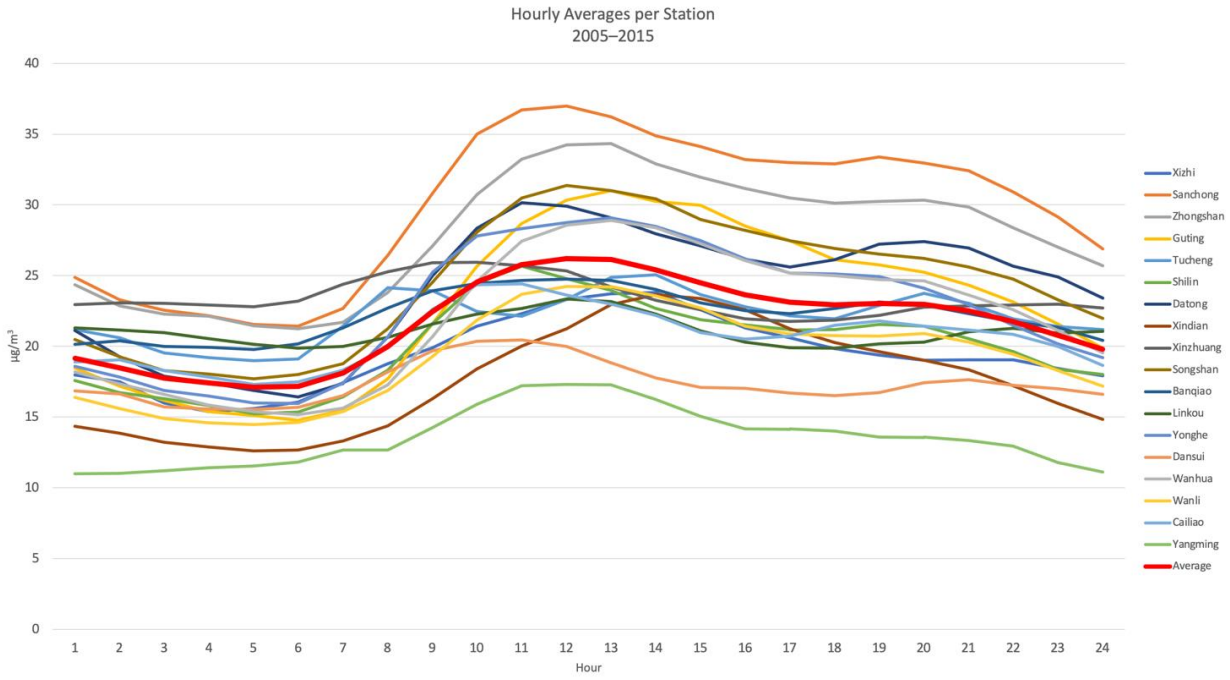

Figure 6: Hourly averages per station in the Taipei Basin from 2005 to 2015

Figure 7: A screenshot from the Taiwan EPA of a map of the air quality stations, along with the corresponding Air Quality Index. The three stations named are the ones discussed in the spatial analysis section.

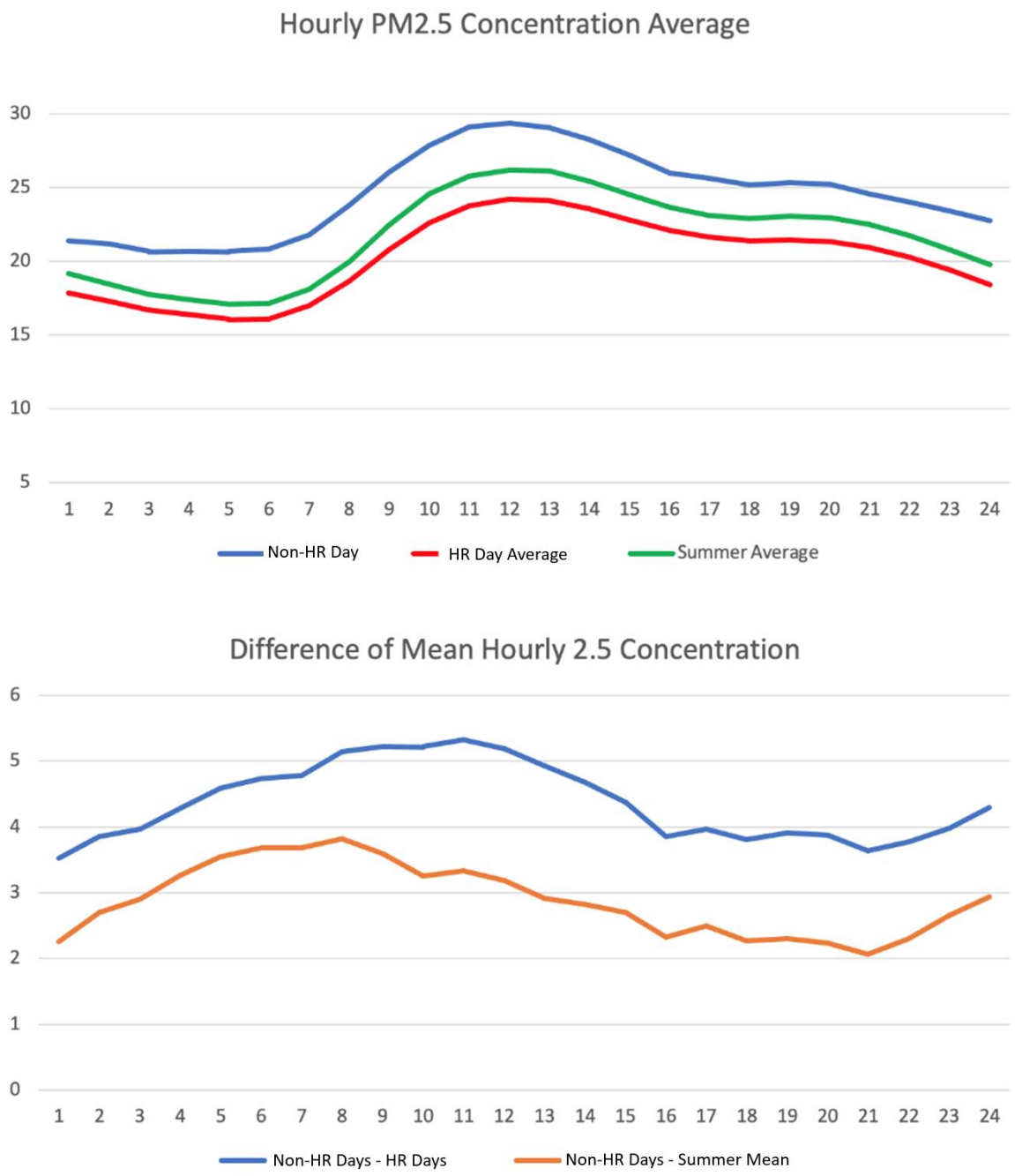

Figure 8: (top) Diurnal cycle of non-HR days, or days with zero rainfall, the summer mean, and the heavy rainfall days. (bottom) The difference between the non-HR days and the summer mean, and the non-HR days and HR days.

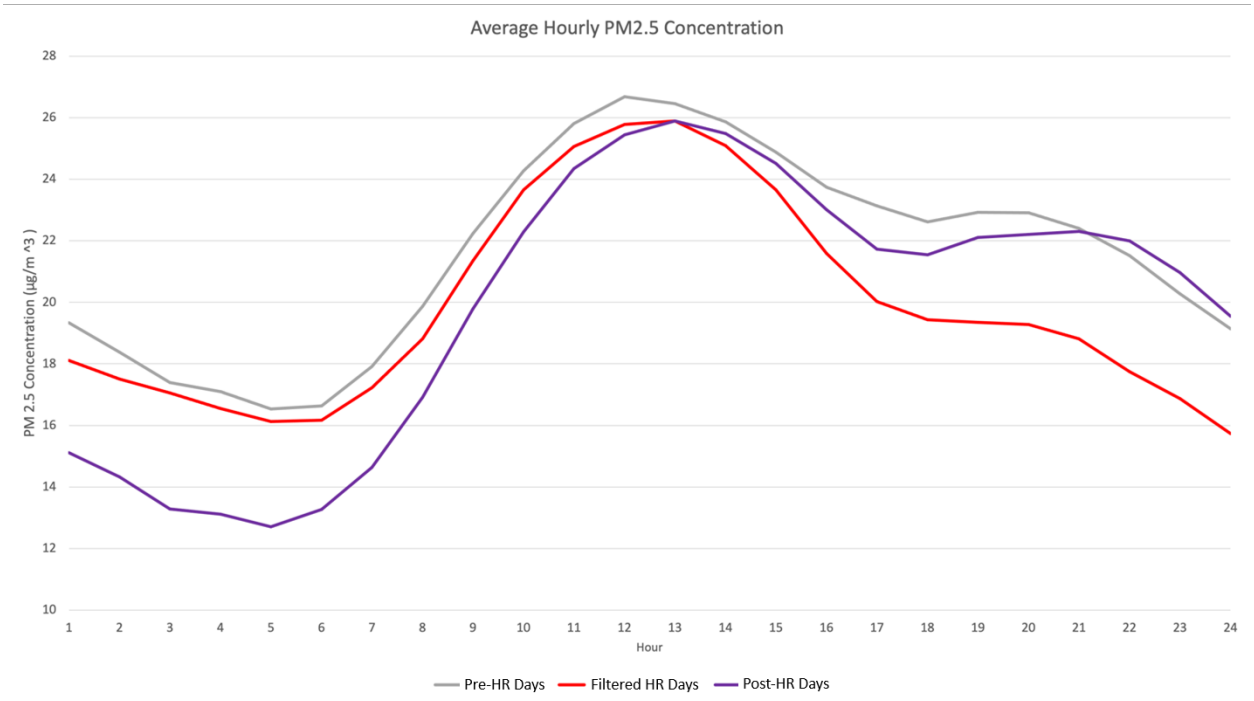

Figure 9: The average diurnal cycle of the days before HR (PRE), the HR days not including consecutive events, and the days after HR (POST)

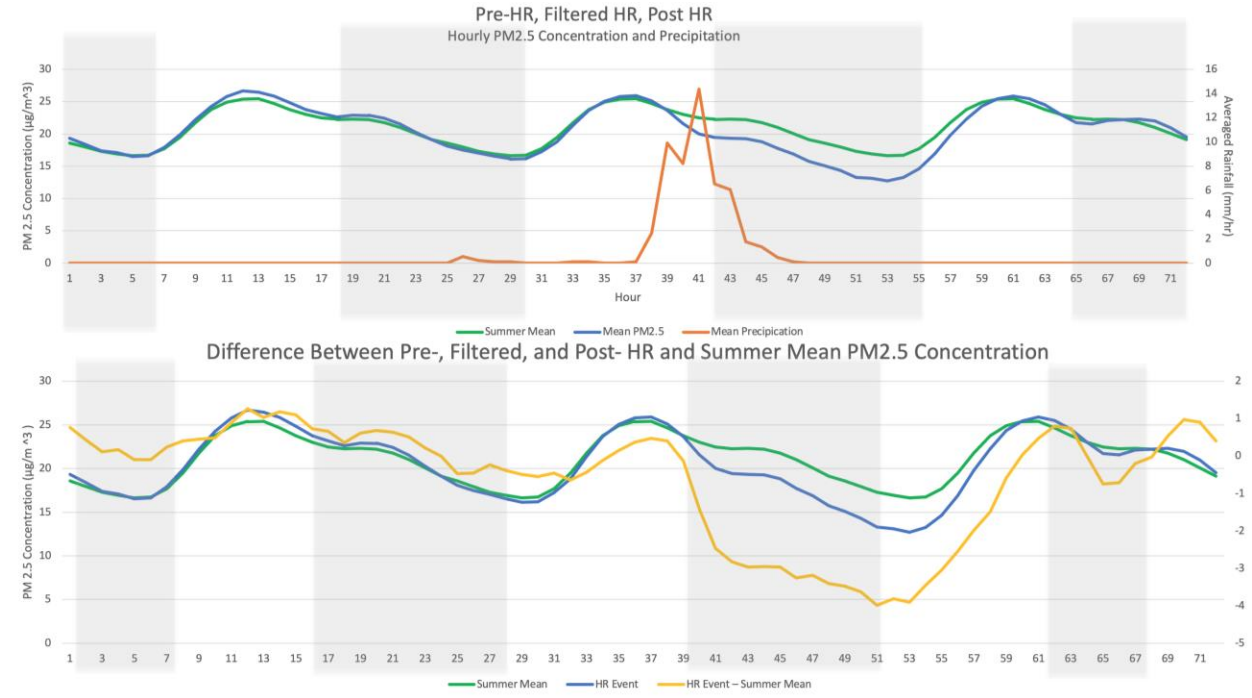

Figure 10: The diurnal cycle of PRE, HR, and POST as a consecutive set, the summer mean, and average rainfall amounts (top). The diurnal cycle of the three days with the summer mean and the difference between the two (bottom).

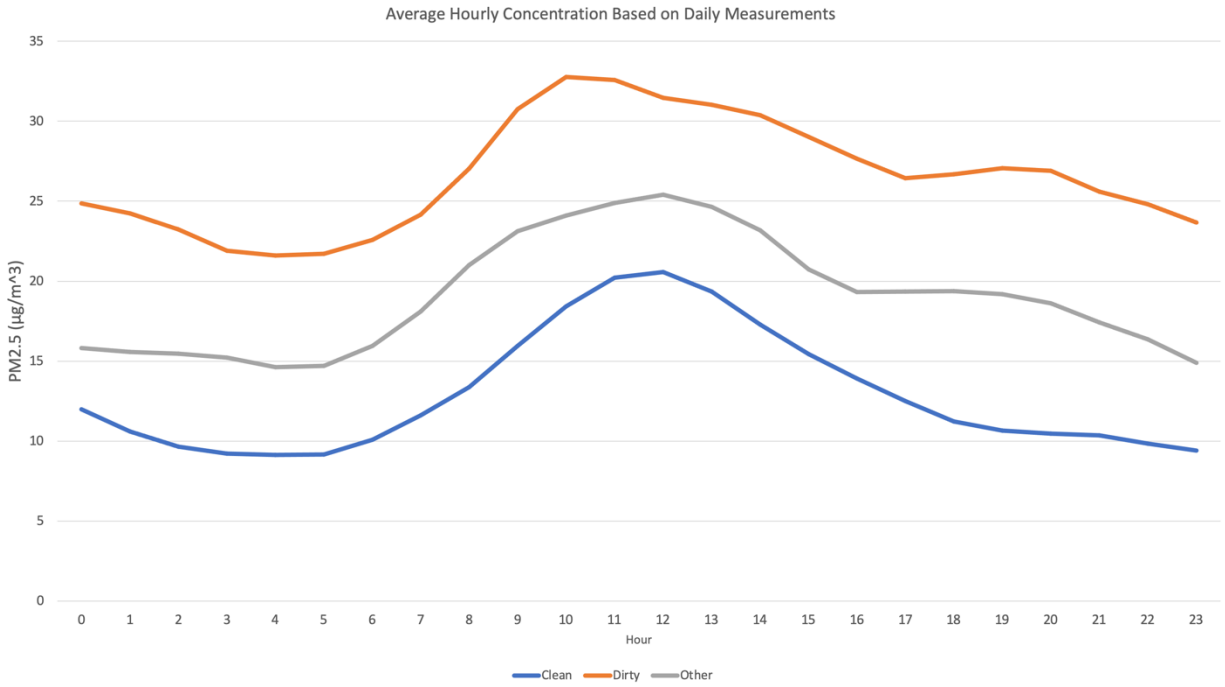

Figure 11: Diurnal cycle of PM2.5 separated by quartiles CLEAN, DIRTY, and OTHER

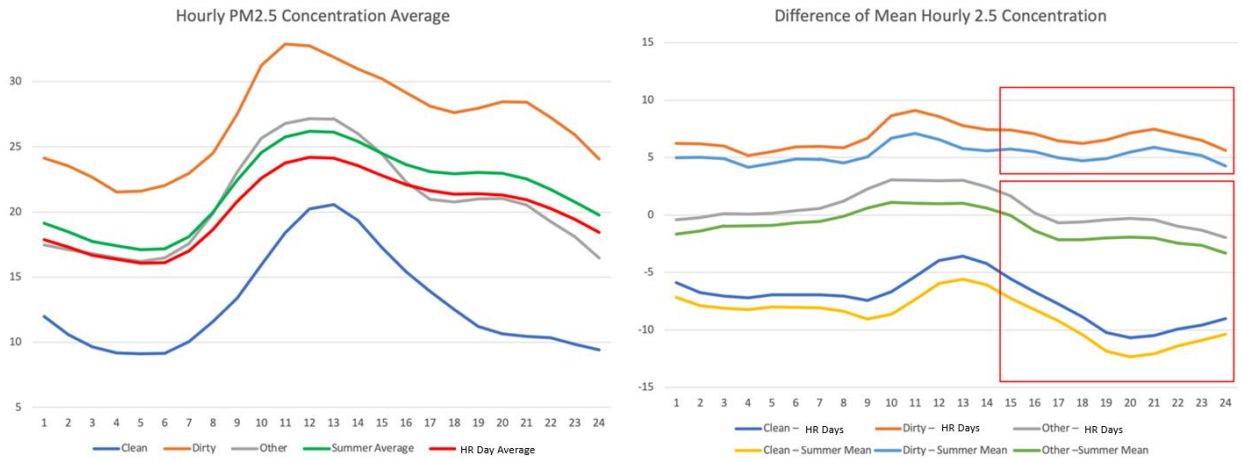

Figure 12: (left) The diurnal cycles of the CLEAN, DIRTY, and OTHER along with the summer mean and the HR average. (right) The difference between the diurnal cycle of each of the quartiles and the summer mean and the HR average.

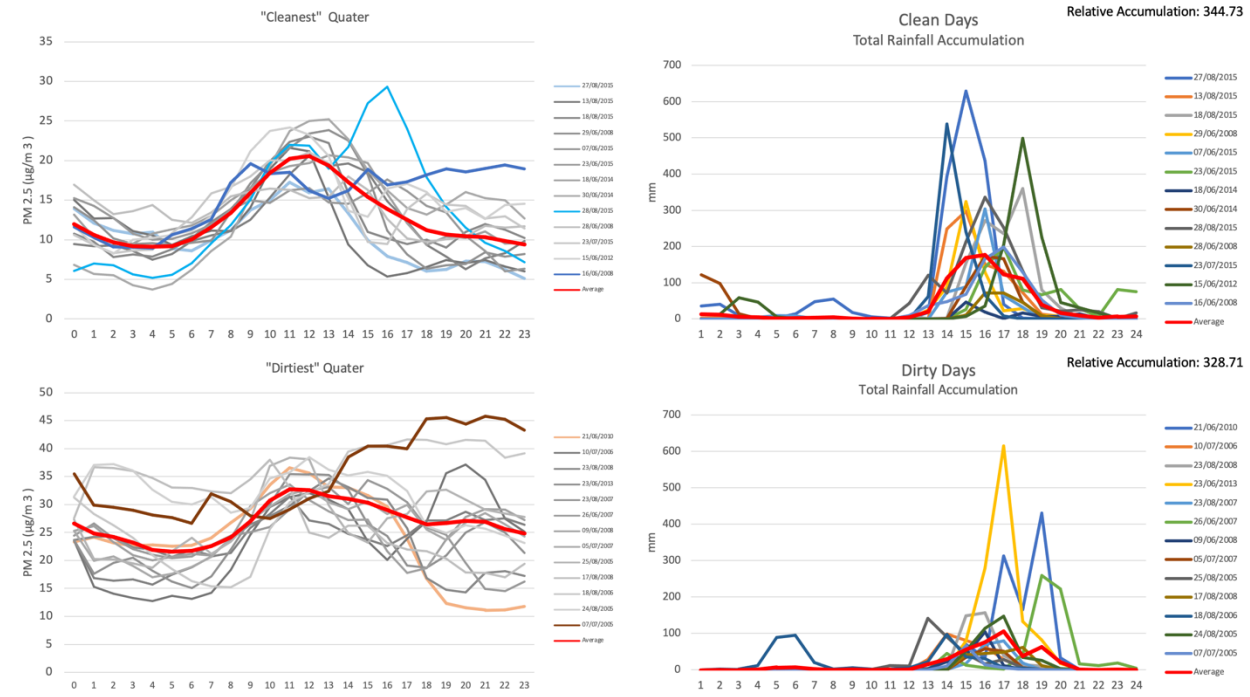

Figure 13: (top) A breakdown of the CLEAN quartile days for PM2.5 and rainfall. (bottom) A breakdown of the DIRTY quartile days for PM2.5 and rainfall.

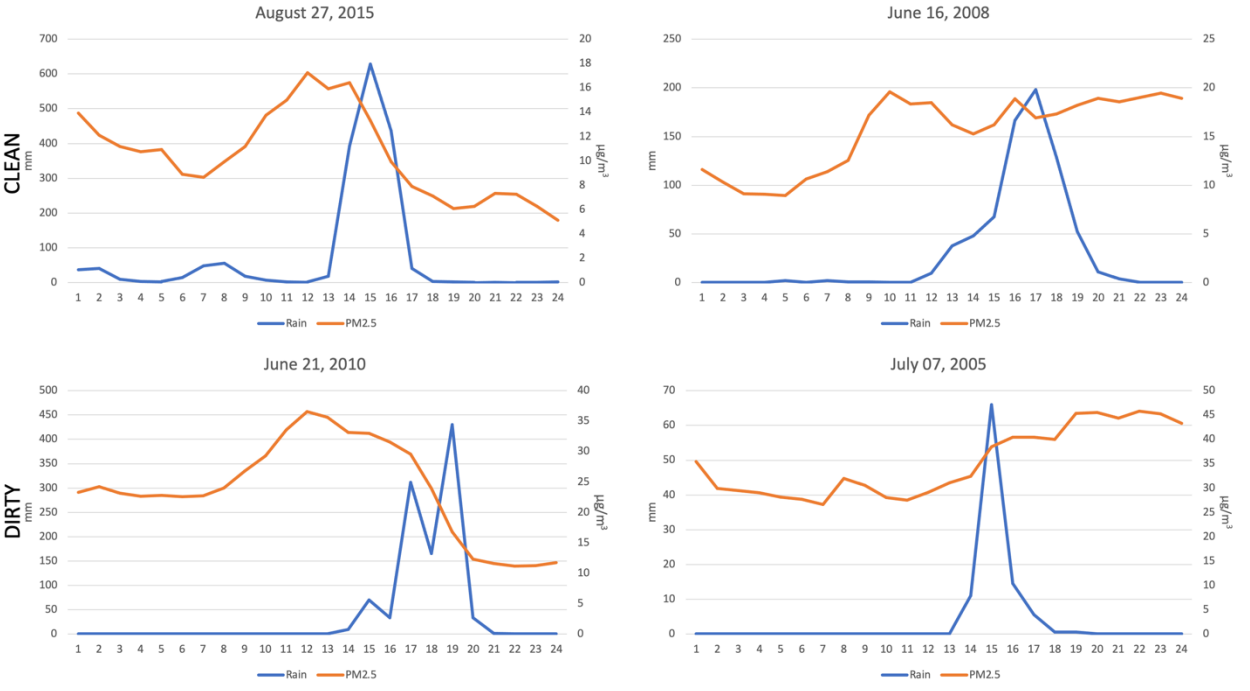

Figure 14: (top left) The day with the lowest PM2.5 concentration in CLEAN. (top right) The day with the highest PM2.5 concentration in CLEAN. (bottom left) The day with the lowest PM2.5 concentration in DIRTY. (bottom right) The day with the highest PM2.5 concentration in DIRTY.

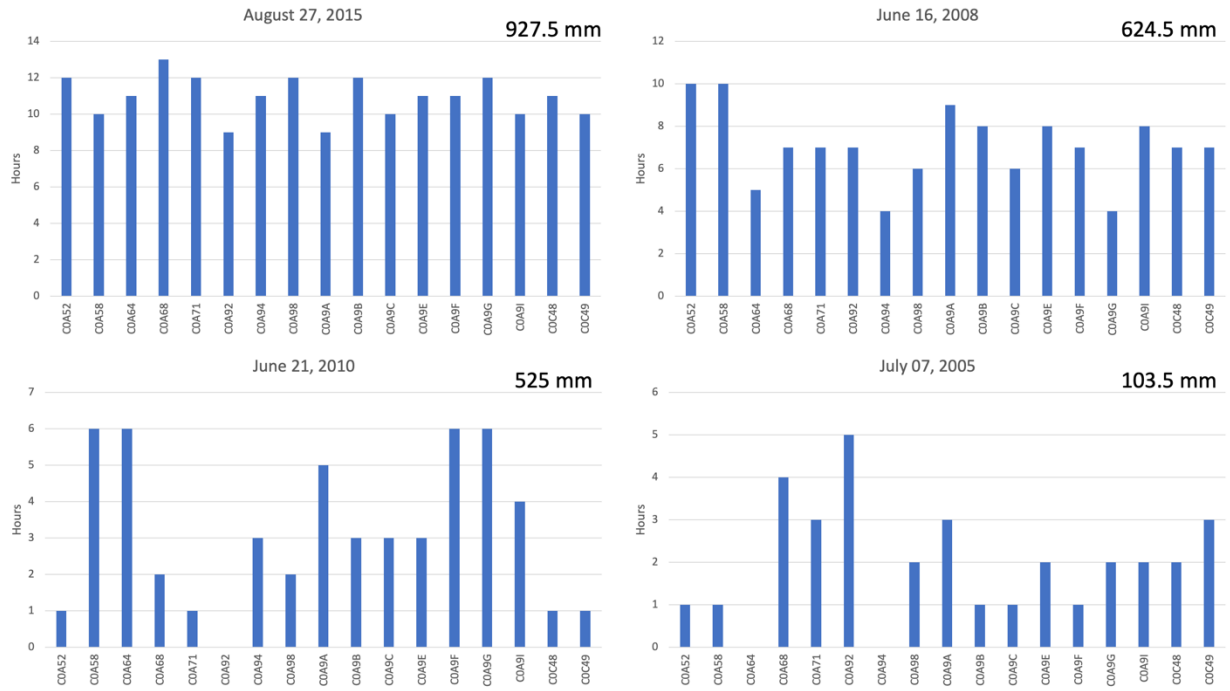

Figure 15: Using only the fifteen stations that are present throughout the whole ten-year period, the number of hours that recorded precipitation. If a station did not record precipitation it is still listed but has no data points. The total precipitation recoded by the stations is on the upper right corner of each graph. Just like ***Figure 14****, each day corresponds to the lowest and highest concentration days in CLEAN and DIRTY.*

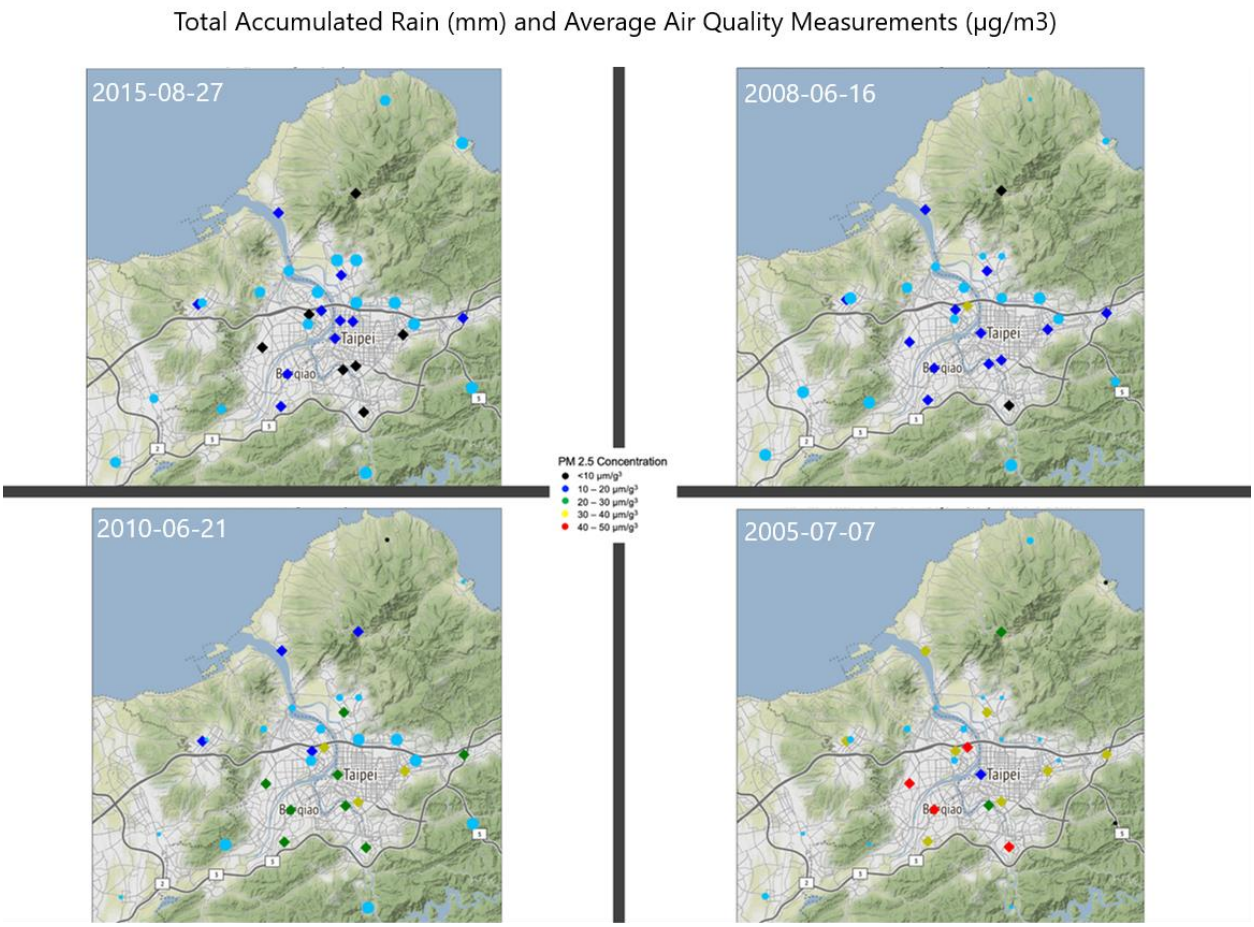

Figure 16: A map of the Taipei Basin with the precipitation stations marked by circles. The stations that recorded precipitation have a blue circle and the size corresponds to the total amount of rain recorded. If a station did not record precipitation, then it is marked by a black circle. Air quality stations are marked by diamonds and the colors correspond to the average PM2.5 concentration.

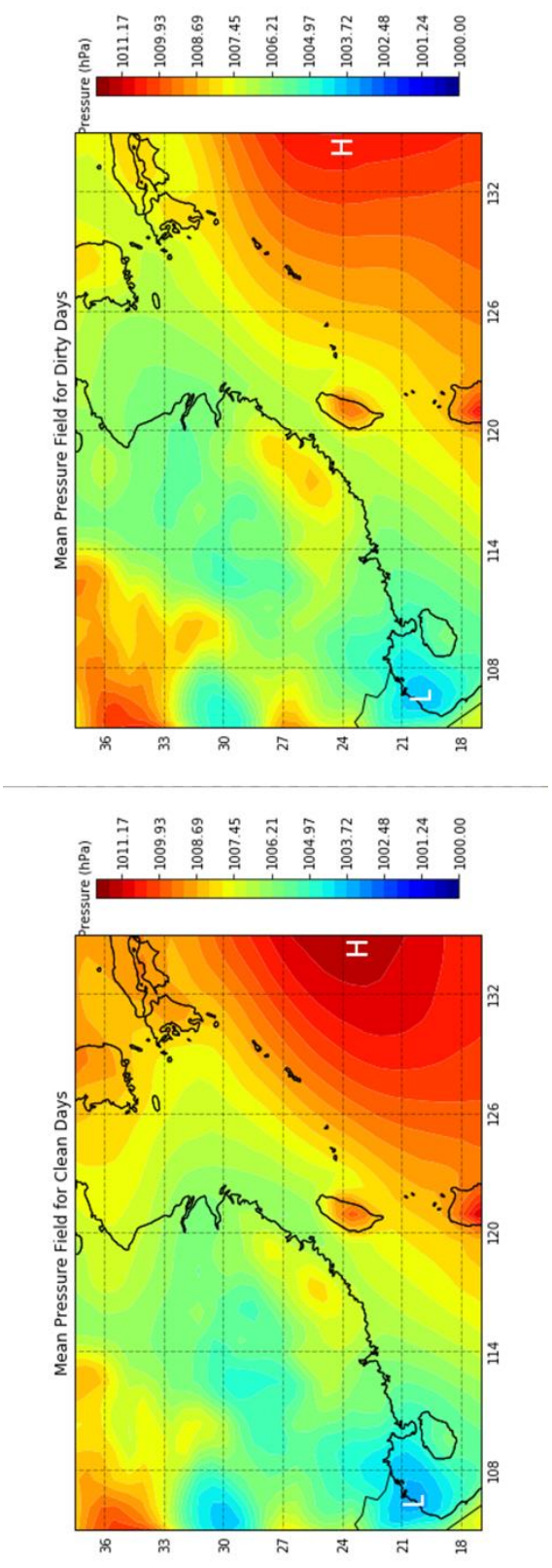

Figure 17: The mean pressure field for CLEAN days (left) and the mean pressure field for DIRTY days (right).

4 Rainfall Analysis– Case Studies

As mentioned earlier, one of the goals of this study is to analyze heavy rainfall events by looking at rainfall characteristics alongside PM2.5 concentrations to see if there is a relationship between the diurnal cycle of both. Case studies of rainfall events provide an additional approach to better understand what the PM2.5 environment looks like leading up to HR events, the effect that heavy precipitation has on PM2.5 concentrations, and how the particulate concentrations can recover after the rain ends. Diurnal cycles are a constant time frame where all background variables are relatively similar (i.e., temperature, radiation, winds), making diurnal cycles the best way to visualize rain's effect on PM2.5 in an observation setting. Perturbations with respect to the diurnal cycle are useful because they highlight points of interest motivating a more detailed study. Further, a detailed study into the location and duration of the precipitation will facilitate the identification of critical characteristics of the heavy rain hotspots such as CWB Heavy Rainfall advisories.

4.1 Mei-Yu Event – June 5-6, 2014

Rainfall characteristics and PM2.5 variations of a Mei-Yu event were analyzed to better understand the uniqueness of the selected heavy rainfall events by contrasting the two types of events. Mei-Yu or Plum Rains are characterized by a stationary front that develops in mid-May to mid-June, typically stretching from southeast China to southern Japan and passing over Taiwan. Very heavy rainfall is often associated with the Mei-Yu front, contributed to by mesoscale convective systems (MCS) as it passes over Taiwan. Over the Taipei Basin and other highly urbanized regions, flash flooding often occurs as the heavy and localized rainfall overwhelms the city sewer systems and the paved roads leave the accumulating rain nowhere to go. On occasion, these flash floods result in a disruption of life and economic losses. While

Mei-Yu events are organized systems that result in relatively localized rainfall due to the size of the front and the duration, there is often heavy rainfall over a much larger region than a local thunderstorm resulting in much higher rainfall totals. Since Mei-Yu events occur every year and have heavy rain, it provides a good benchmark for severe rainfall characteristics and impacts on PM2.5 concentrations.

Similar to most Mei-Yu events, the event on June 5-6, 2014 had a stationary front extending from southern China, across the Taiwan Strait, and over northern Taiwan, resulting in two days of heavy rainfall over northern Taiwan. Figure 18 shows the hourly concentration averaged across all stations (red) in the Taipei Basin starting on June 4th, as well as the summer background mean introduced in the earlier section (green), and the hourly precipitation averaged across all stations (blue). June 4th and June 5th show a consistent increase in PM2.5 leading up to the front passing over the Taipei Basin and heavy rainfall beginning. By 12 LST on June 5th, the PM2.5 concentration is 35.96 μg/m3, about 10 μg/m3 higher than the summer mean.

Rainfall begins at 13 LST and becomes heavy between 22 and 23 LST. The heavy rain in the latter part of the day likely plays a significant role in the sharp decline in the hourly concentration of PM2.5. Figure 19 shows a snapshot of 2 LST on June 6th, the second day of heavy rainfall, when it is both the minimum in average PM2.5 and a rainfall maximum. The CWB radar on the bottom left shows the rainfall passing over the basin. The map on the right shows that every single station is recording precipitation, with several stations recording 10 or 20 mm/hr (based on dot size), further illustrating the spatial extent of the precipitation. The fact that both the maximum in rain and minimum in PM2.5 concentration happen concurrently emphasizes the idea that rainfall and washout directly impact the particulate concentration over the basin. The difference in rainfall and PM2.5 concentration at that particular moment serves as

an important reference point when looking at HR events and how PM2.5 concentrations react to precipitation. While in six hours of heavy rain, the PM2.5 concentration fell 23 μg/m3, the following seven hours had an impressive recovery rate of about 3.6 μg/m3 (about +0.5 μg/m3 per hour) By 10 LST on June 6th, the particulate concentration peaked at 33 μg/m3, a total increase of 25 μg/m3 since the early morning. The dynamics of mesoscale circulations may have caused a strong surge in particulates. As convective cells pass through the region, downdrafts and storm outflow can create strong currents near the surface, picking up particulates and mixing them into the atmosphere along with those emitted in the urban setting.

After the PM2.5 concentration recovers, the concentration decreases sharply on the nights of June 6th and June 7th. Washout alone is not likely to have been the singular cause for the sharp declines. Instead, a combination of storm flow moving into the basin and the onset of the local land breeze provided ideal ventilation in the basin, similar to the findings in Chen et al. (2014). Both sharp declines after precipitation and the recovery rates in PM2.5 concentration provide insight into how HR events can impact particulate concentration and what can be expected during the case study analyses. Further analysis was conducted to better understand what the rainfall was like during the Mei-Yu event and its impact on PM2.5 concentrations. Figure 20 shows station frequency tables for three of the four days analyzed (because the first day did not have any rainfall). On average, 32 stations recorded precipitation for 7 hours. Given that there were 32 stations recording precipitation, that means that the rainfall was widespread throughout the whole basin for an average of 7 hours. Knowing the extent and duration of precipitation is important because it gives an idea of how many places were possibly experiencing washout and how long (impacting the decline rates of PM2.5).

Rainfall totals and duration at each station were analyzed to get a complete picture of the precipitation severity across the basin. Figure 21 shows the total accumulated rainfall per station for each of the three days with rainfall. CWB Heavy Rain Advisory descriptions (https://www.cwb.gov.tw/V8/E/P/Warning/W26.html) were used to gauge the severity of the rainfall. On June 5th, two stations met the criteria for a heavy rainfall advisory (C0C48 exceeded 40 mm in one hour, C0AH0 exceeded 80 mm in 24 hours), and on June 6th four stations met the criteria for a heavy rainfall advisory (C0ACA, C0AH1, C0C49, C0C64 exceeded 80 mm of rain in one hour, C0C64 exceeded 40 mm in 24 hours). On the last day of analysis, none of the stations met the criteria for a CWB advisory. Despite a large amount of rainfall falling for an extended period, only a few stations were considered to have heavy rain.

4.2 Single Heavy Rain Event– June 14, 2015

The synoptic environment on June 14, 2015, was very similar to the mean pressure field of all the HR days with general low pressure to the west and southwest, and higher pressure to the north and southeast with a stationary front extending from south-central China towards the Korean peninsula (Figure 22). June 14, 2015 is a well-documented summer afternoon thunderstorm in the Taipei Basin because of its intense rainfall rate and urban flooding. Miao and Yang (2020) describe how the weak synoptic environment and weak convective instability that preceded the storm were changed by the interaction of sea breeze circulation. Since most of the forcing for the convective development of this storm was local, it provides a real case example of an ideal environment for precipitation and PM2.5 analysis.

An hourly analysis of the precipitation provides insight into the PM2.5 response to intense precipitation and can be compared to Figure 10 (PM2.5 section) where all the HR days are averaged. Figure 23 shows Figure 10 (top) and the hourly PM2.5 concentration, PM2.5 summer

mean, and average hourly rainfall for June 13–15, 2015 (bottom). Since the summer mean works as a background constant that HR events are happening in, it is useful to see how the PM2.5 trends on a particular HR day may vary from the background state. The PM2.5 concentration for the three days of the June 14th HR event is always below the summer background mean. The biggest impact that precipitation has on the particulate concentration is when there is rainfall. Three hours after the HR event begins (around 17 LST) about 10 μg/m^3 of particulates have been washed out by precipitation. At this point, the difference between the hourly concentration and the summer mean is the greatest (a difference of about 11 μg/m^3). Despite the latter part of the storm continuing, the PM2.5 concentration began to increase so that at 23 LST there was a second peak of 15 μg/m^3, but by this point, the difference between the two concentrations was only about 4 μg/m^3. This difference remains more or less constant for a couple of hours so that both reach a minimum at 4 LST on June 15th and then begin to rise.

After analyzing and understanding the pattern of PM2.5 and its response to heavy rain, the hourly concentration of this single-day HR event can be compared to the filtered HR days. It is easier to understand how both hourly concentrations are deviating from the background state since both are being compared to the same background summer mean. The averaged concentration of the filtered HR days is more like the summer mean, deviating only slightly during the peak of each day and when precipitation occurs (Figure 23). The hourly concentration of the single-day HR event starts at a lower concentration and never really manages to reach a concentration as high as the summer mean. However, one of the key similarities in both situations is the response that PM2.5 has to precipitation. In both cases, the largest deviations from the summer mean occur when rainfall and washout decrease the concentration. Yet, the recovery rates after the rain are like those of the summer mean. Unlike the HR averaged

concentration, the hourly concentration on June 15th does not recover to pre-rainfall values and remains constant throughout the day.

The spatial and temporal distribution of the precipitation was analyzed to better highlight the spatial extent of the storm and how long it lasted. Since there was precipitation the days before and after the HR event, all three days were analyzed (Figure 24). On June 13th there was rainfall across ten stations for an average of 2.3 hours. On June 15th there was rainfall across five stations for an average of 1.6 hours. In contrast, on June 14th during the HR event, there was rainfall across 24 stations for an average of 3.6 hours, with two stations recording rainfall for 6 hours. While 6 hours of rain at two stations may seem like a long time, the Mei-Yu event recorded precipitation at all stations (32) for an average of seven hours, more than twice the average time of the single HR event. This shows that while the origin and characteristics of the two storms are different, a locally thermodynamically produced storm can still produce rainfall over a widespread area, though it may not last as long. The precipitation the day before (June 13th) shows what a more "regular" or weak rainstorm looks like in terms of area covered and average duration.

To understand the severity of the precipitation, the total accumulated rainfall was measured for each of the stations that recorded precipitation and the CWB Heavy Rain Advisory regulations were used as an objective risk assessment (Figure 25). On June 13th, the day before the HR event, there was some precipitation and it did not last a long time, nor was it significantly extensive. Two (C0AC7 and C0AC8) stations received more than 40 mm of rainfall in an hour, classifying as a Heavy Rain Advisory. One of those stations (C0AC8) also met a second Heavy Rain Advisory condition as its 24-hour total exceeded 80 mm of rain. On June 14th, the day of the HR event, three stations (C0A9A, C0AC8, and C0AH1) recorded more than 40 mm of rain in

an hour. Two of those stations (C0AC8 and C0AH1) also recorded over 80 mm of rain in 24 hours to classify as a Heavy Rain Advisory. In addition, two stations (C0AC7 and C0AG9) had a 3-hour accumulated rainfall exceeding 100 mm, classifying as Extremely Heavy Rain Advisories. Compared to the Mei-Yu event where four stations had Heavy Rain Advisories, only three stations met the same criteria. However, two stations recorded even more intense precipitation reflecting a possibly stronger convective event despite being a locally forced storm. In the two-day Mei-Yu event, there was also only one station in one of the days that exceeded a total of 100 mm, while in the HR event on June 14th, there were four stations that either met or exceeded an accumulated total of 100 mm, further showing that despite being a locally forced storm, the precipitation was much stronger. The day after the HR event the stations only had some light rain, with the maximum accumulation at C0AH0 of just 3.5 mm. There were no significant precipitation recordings on this day.

4.3 Three Heavy Rainfall Events – June 21-23, 2010

From June 21st to June 23rd, 2010 there were three days of heavy rainfall events in a row. This means that during each day there was an afternoon thunderstorm that met the HR criteria. From the whole set of data across the ten years, there is only one case that has three days in a row recording significant precipitation, making it a special case worthy of further analysis.

While the background synoptic state was very similar to the mean composite, with high pressure to the east and a stationary front to the north (Figure 26), the PM2.5 concentration on the first day is one of the highest of the dataset, making it part of the DIRTY set of days analyzed in the PM2.5 section. Apart from being a unique case because of the three convective days in a row, having a high PM2.5 concentration before the rain begins also provides insight not only into how the PM2.5 responds to the rainfall but also how the PM2.5 concentrations relate to the mean

background state. An hourly analysis of the PM2.5 concentration, the PM2.5 background summer mean, and the average hourly precipitation is displayed in Figure 27. The day before the HR event on June 20th, the hourly concentration is very similar to the summer mean initially but by nighttime, the concentration begins to rise and continues to do so until 11 LST on June 21st. By this point, with a concentration of 32.95 μg/m^3, the hourly concentration was almost 10 μg/m^3 higher than the summer mean. Almost immediately after 11 LST when rainfall began the hourly concentration decreased at a steep rate. When the rainfall peaked at 17 LST the PM2.5 concentration was already half (15 μg/m^3) of what it had been six hours prior and 5 μg/m^3 below the summer mean. Like the previous two cases discussed, the highest PM2.5 concentration is recorded right before precipitation begins and then decreases as soon as the precipitation begins.

Besides sharing the PM2.5 characteristics when precipitation begins, on June 22nd and June 23rd the hourly concentration shows an impressive recovery despite washout from precipitation. After the precipitation ended on the night of June 21st, the PM concentration remained relatively constant (~10 μg/m^3) for about 8 hours with washout and ventilation removing most of the particulates in the air. The concentration then increases sharply so that within four hours, at 9 LST on June 22nd the PM2.5 concentration is reaching its first peak of the day at 22 μg/m^3. After precipitation in the mid to late afternoon, the hourly concentration decreases back to about 10 μg/m^3, only to have another impressive recovery over 12 hours to 24 μg/m^3. At this point, the hourly concentration is equal to the summer mean measurement for that hour. It is possible that convective cells approaching the region can create strong currents near the surface, picking up particulates and mixing them into the atmosphere and that is why before precipitation begins, there is a surge in particulates recorded throughout the Taipei Basin.

With the temporal analysis of the precipitation and PM2.5 concentrations giving a picture of the sequential development throughout the five days, station frequency tables were created to understand the temporal and spatial distribution of the precipitation (Figure 28). On June 21st, the first HR day, it rained for an average of 3.5 hours across 26 stations. All the stations that recorded precipitation for six hours or more are located on the eastern part of the Taipei Basin at the foot of elevated terrain. Like the one-day event analyzed in the previous section, the precipitation averages about 3 hours across different stations but has a large range in precipitation duration, unlike the Mei-Yu event. On June 22nd, it rained for an average of 4 hours across 21 stations. There were fewer stations that had six hours of rainfall, though the ones that did record for six hours were among the same stations that precipitated for six hours the day before. There was also a group of stations in a similar vicinity in the urban center of Taipei City that recorded precipitation for five hours. This urban center is one of the areas that tend to have higher PM2.5 concentrations, suggesting that there are a lot of particulate emissions in this area as well. The precipitation trends of these two days are different from that of June 23rd. On the third and last HR day, there was precipitation recorded at 24 stations for an average of 2.5 hours, with only one station recording for six hours. From the amount of time that was recorded across the stations, it does not seem like this HR event was as severe as the previous HR events analyzed and is even more different than the scenario presented in the Mei-Yu event.

June 24th is not an HR event, but there is some precipitation recorded. It is still valuable to analyze the precipitation patterns of the day since it still relates to the recovery rates of PM2.5 after HR events. Precipitation was recorded at 29 stations for an average of three hours. On this day there were more stations recording precipitation than the previous three days and the duration was more constant across the stations. This presents a picture of a light rain (or

"regular") event, rather than a heavy rain event that could be more localized and potentially last less time but have a higher rainfall rate leading to larger accumulations. Like the rainfall analysis of June 15, 2015, June 24th serves as a benchmark for what more common and less severe rainfall looks like, further highlighting the unique characteristics of HR events.

Looking at the accumulation of rainfall at each station through the course of the three days provides a way to see the severity of the storm at different points referencing the station frequency tables (Figure 29). On June 21st seven stations recorded precipitation for six hours or more (Figure 28) and four of those stations met the CWB Heavy Rain Advisory criteria. Stations C0A9F, C0AC8, and C0AD2, all located in the eastern part of the basin, exceeded 40 mm in an hour, meeting one of the criteria for a Heavy Rain Advisory. Stations C0AD2 and C0AC7 exceeded 80 mm of rain over 24 hours to meet the Heavy Rain Advisory. Apart from these four stations, C0A52 in the southwestern part of the basin also met the criteria for Heavy Rain. Although it only rained for one hour, rainfall exceeded 40 mm. Station C0AD4 recorded precipitation for a total of four hours (Figure 28) and within three hours more than 100 mm of rain were recorded meeting the criteria for an Extremely Heavy Rain Advisory. Three stations (C0A64, C0AC8, C0AD2) recorded more than 80 mm of rain on June 22nd and were classified as Heavy Rain. Two of these stations (C0AC8, C0AD2) had met the criteria for Heavy Rain Advisories the previous day as well. C0AC8 also met the other criteria for a Heavy Rain Advisory of exceeding 40 mm of rain in one hour. All three stations recorded precipitation for a total of six hours.

On June 23rd, none of the stations had a rainfall rate that met the criteria for an advisory. Only 9 out of 24 stations recorded more than a couple of millimeters of rain and all these stations were nestled in the eastern region of the basin near elevating topography. The station (C0A64)

that recorded precipitation for the longest (6 hours) was also the same station that recorded the most rain, for a total of about 60 mm. June 24th recorded precipitation across many stations (29) for a similar amount of time on average (3 hours) but when the total accumulations are analyzed the totals are very low, with the maximum of 11 mm being at C0AD2. This paints a picture of light rain across a widespread area, rather than strong convection with large rainfall rates in a concentrated region like the HR events or large rainfall rates across a large region like the Mei-Yu event.

4.4 Summary

The case studies provide a snapshot of the impact that precipitation has on PM2.5 concentrations and characteristics of the rainfall on HR events and other rainfall events that frequently occur in the Taipei Basin. The case study analysis highlights the impact that precipitation has on PM2.5 concentration. However, the impact that various PM2.5 concentrations can have on convective development and rainfall characteristics is unclear. Differences in precipitation duration and rainfall rates show characteristics of HR events and serve as an observation benchmark for modeling experiments discussed in the following section. A summary of the key points from this section are

1. The effect of rainfall on PM2.5 via washout became very clear in the hour by hour precipitation-PM2.5 comparison plots (Figures 18, 23, 27).
2. Comparing a Mei-Yu event to HR events there are clear differences in rainfall characteristics. The spatial extent of Mei-Yu events is larger, while the rainfall rates of HR events can be higher (noted by differences in CWB classifications).

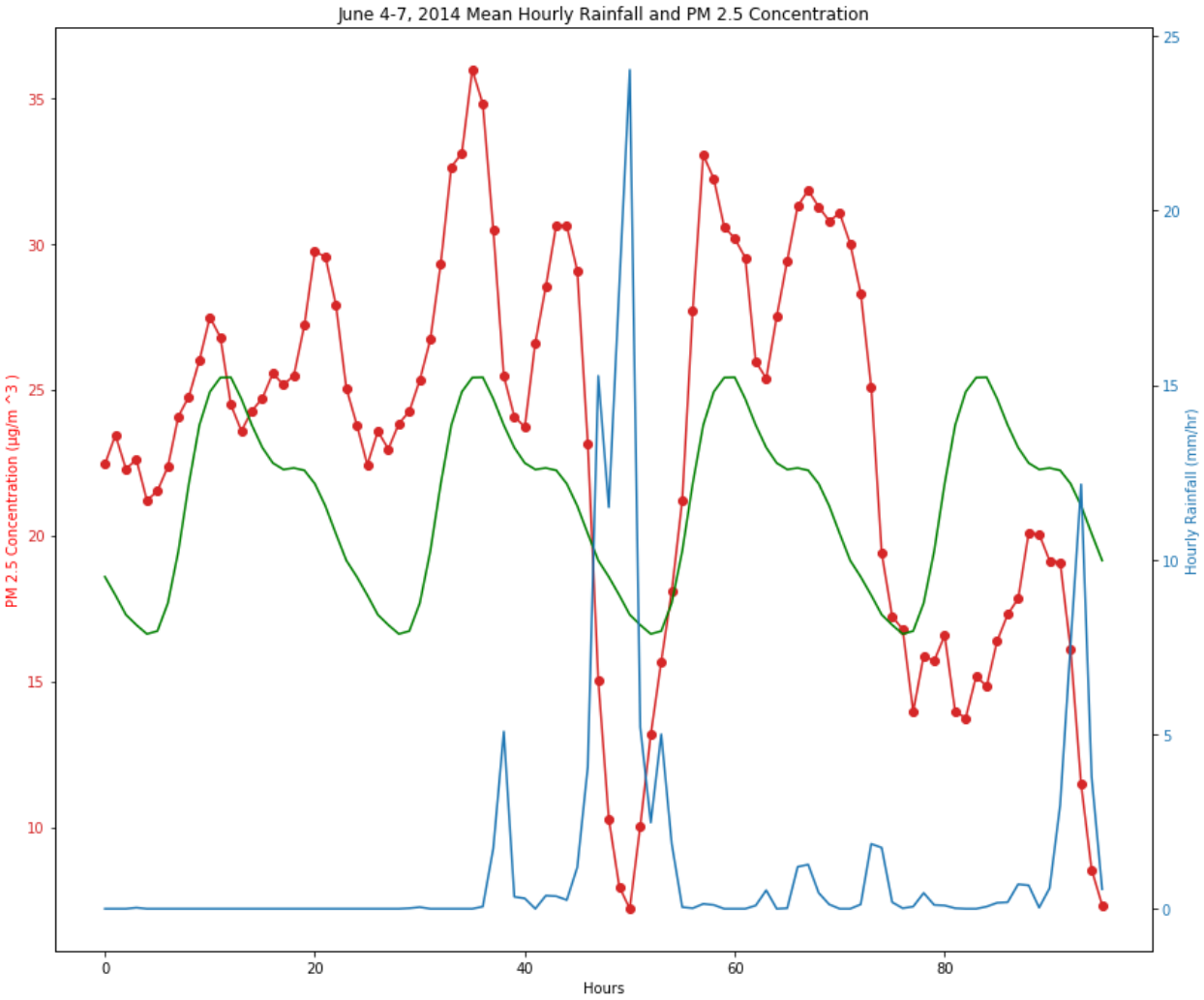

Figure 18: The hourly average PM2.5 concentration from June 4 to June 7, 2014 (red), the summer mean (green,) and the accumulated hourly rainfall averaged across all the stations in the Taipei Basin (blue).

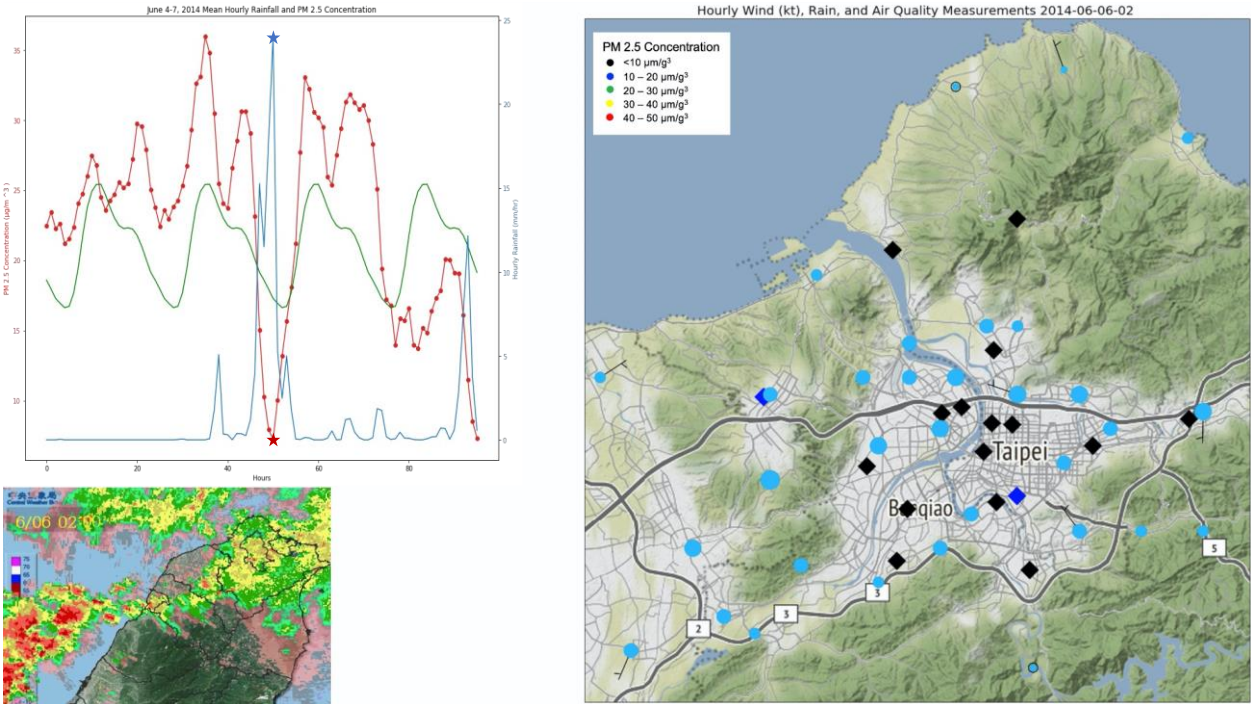

Figure 19: The top left figure is the same as Figure 18, highlighting the rain and PM2.5 concentration at 2 LST on June 6, 2014. The bottom left image is a snapshot of the CWB radar for the same time, showing the precipitation over northern Taiwan. The image on the right shows the stations recording rainfall and the amount for the hour (dot size), as well as the PM2.5 station measurements.

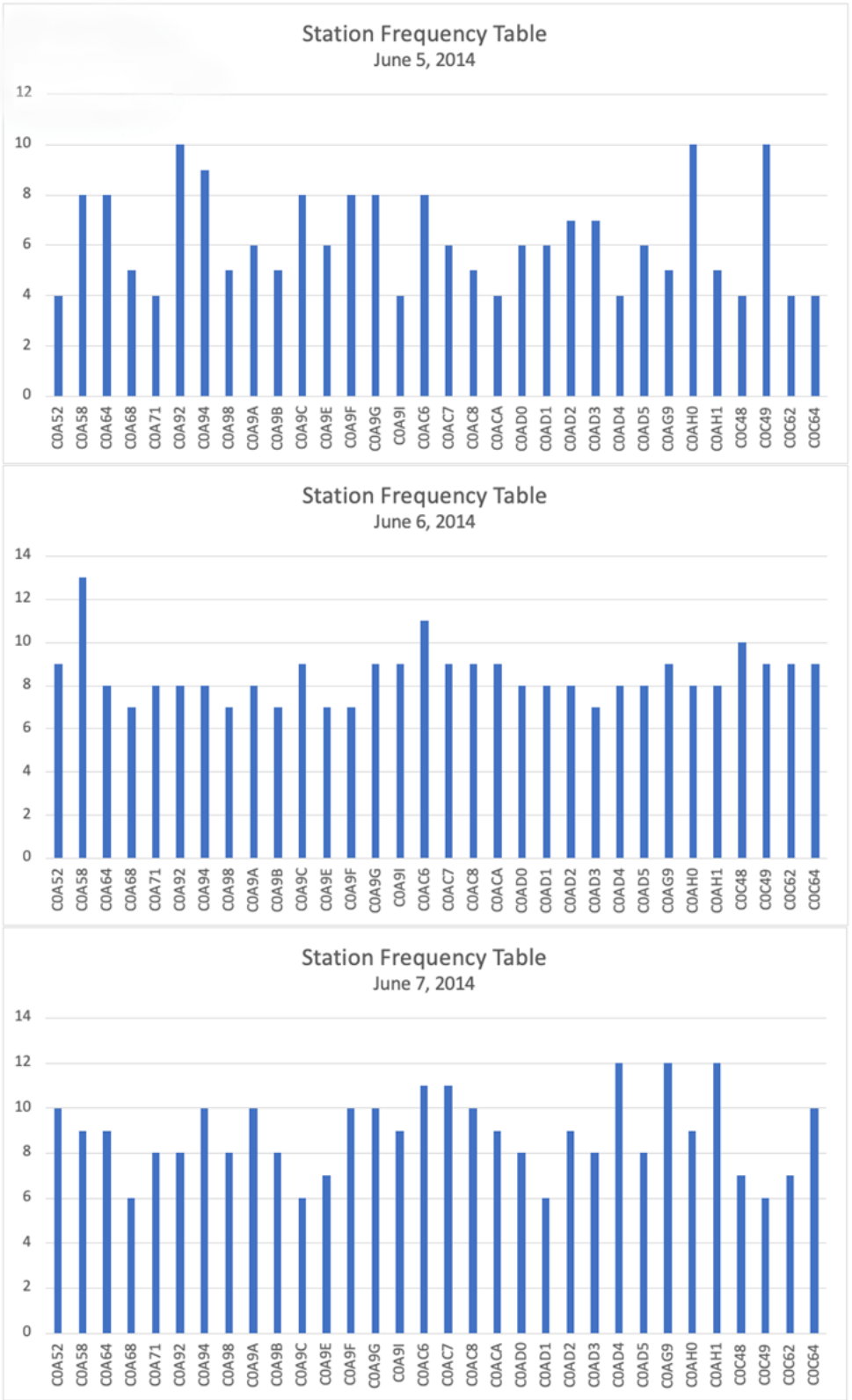

Figure 20: The stations recording rainfall and the total number of hours that rainfall was recorded at each station.

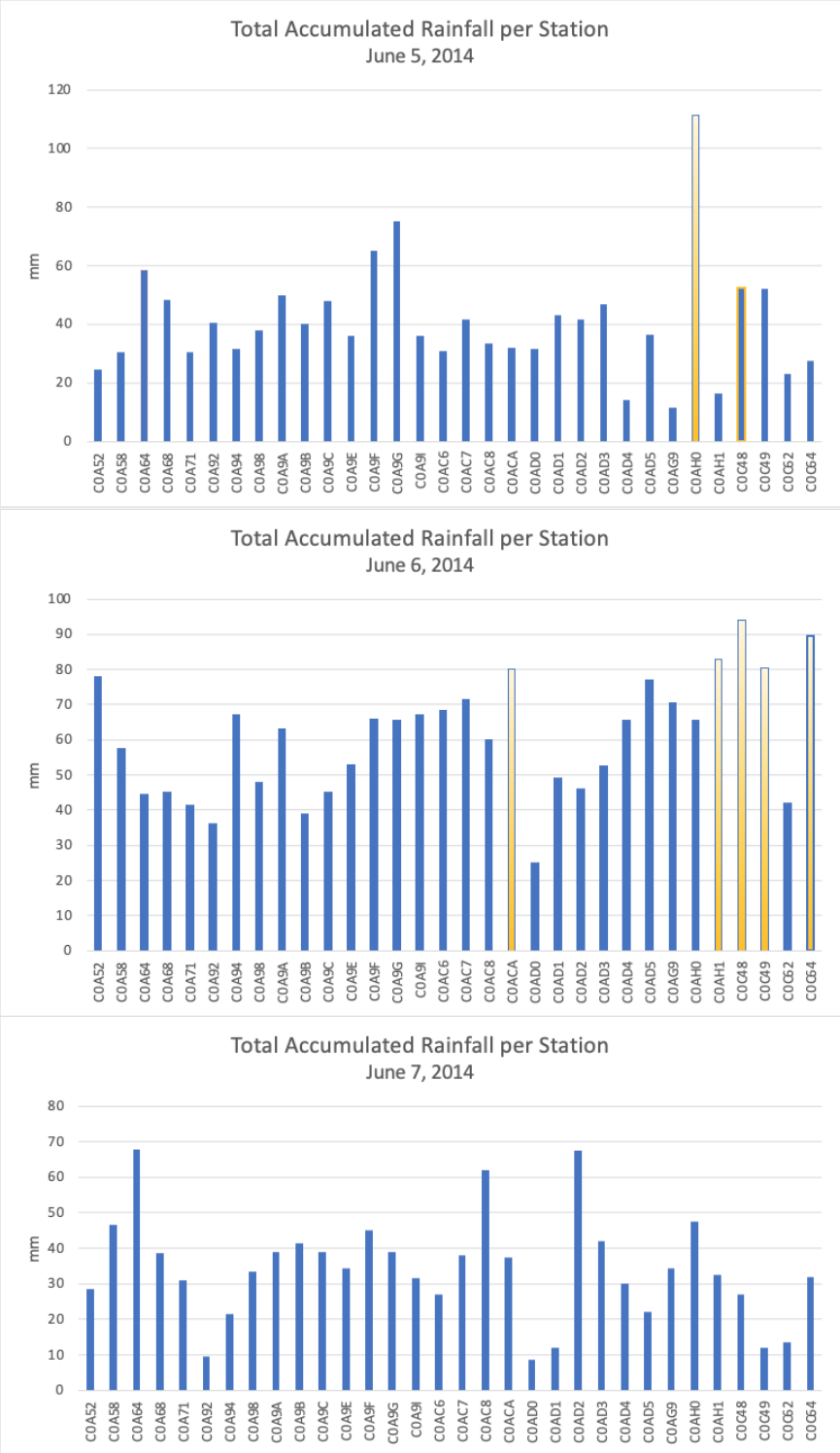

Figure 21: Total accumulated rainfall per station. A yellow outline means the 1-hr rainfall exceeds 40 mm, meeting the criteria for heavy rain advisory according to the CWB. A yellow fill means the 24-hr accumulated rainfall exceeds 80 mm, also meeting the criteria for a heavy rain advisory according to the CWB.

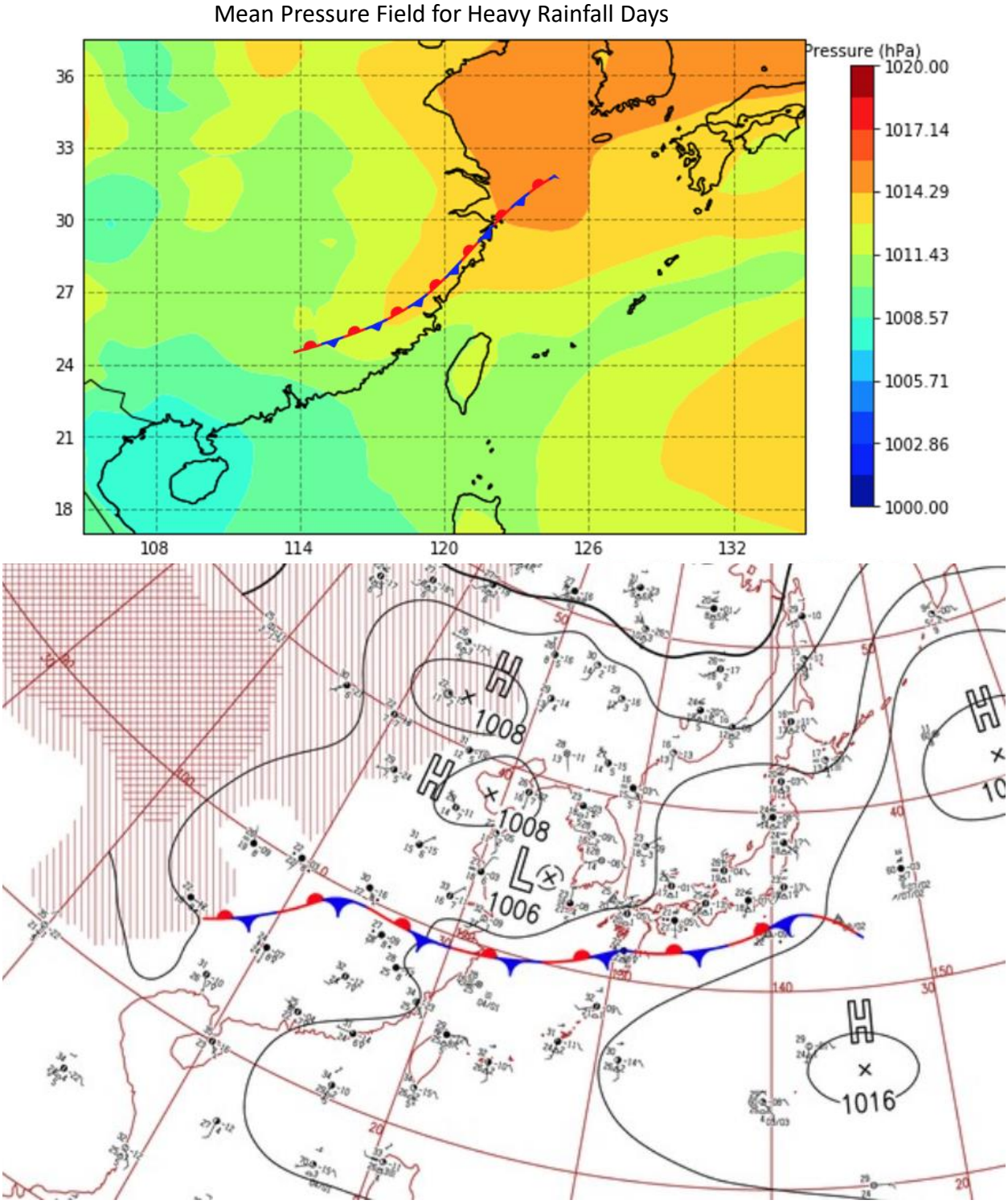

Figure 22: The mean pressure field for all the HR days (top) and a surface map from the Japan Meteorological Society of June 14, 2015 depicting a similar synoptic environment (bottom – Created by National Institute of Informatics "Digital Typhoon" based on "Weather Charts" from Japan Meteorological Agency).

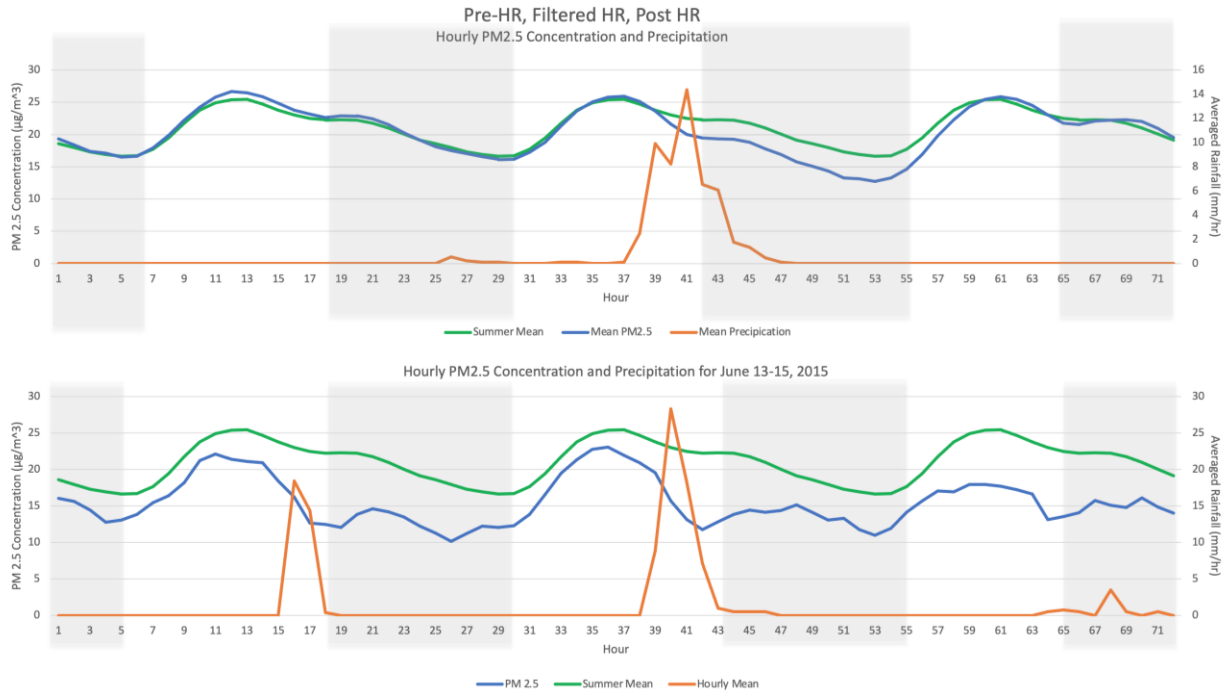

Figure 23: The diurnal cycle of PRE, HR, and POST as a consecutive set, the summer mean, and average rainfall amounts (top). The hourly average PM2.5 concentration from June 13 to June 15, 2015 (blue), the summer mean (green) and the accumulated hourly rainfall averaged across all the stations in the Taipei Basin (orange).

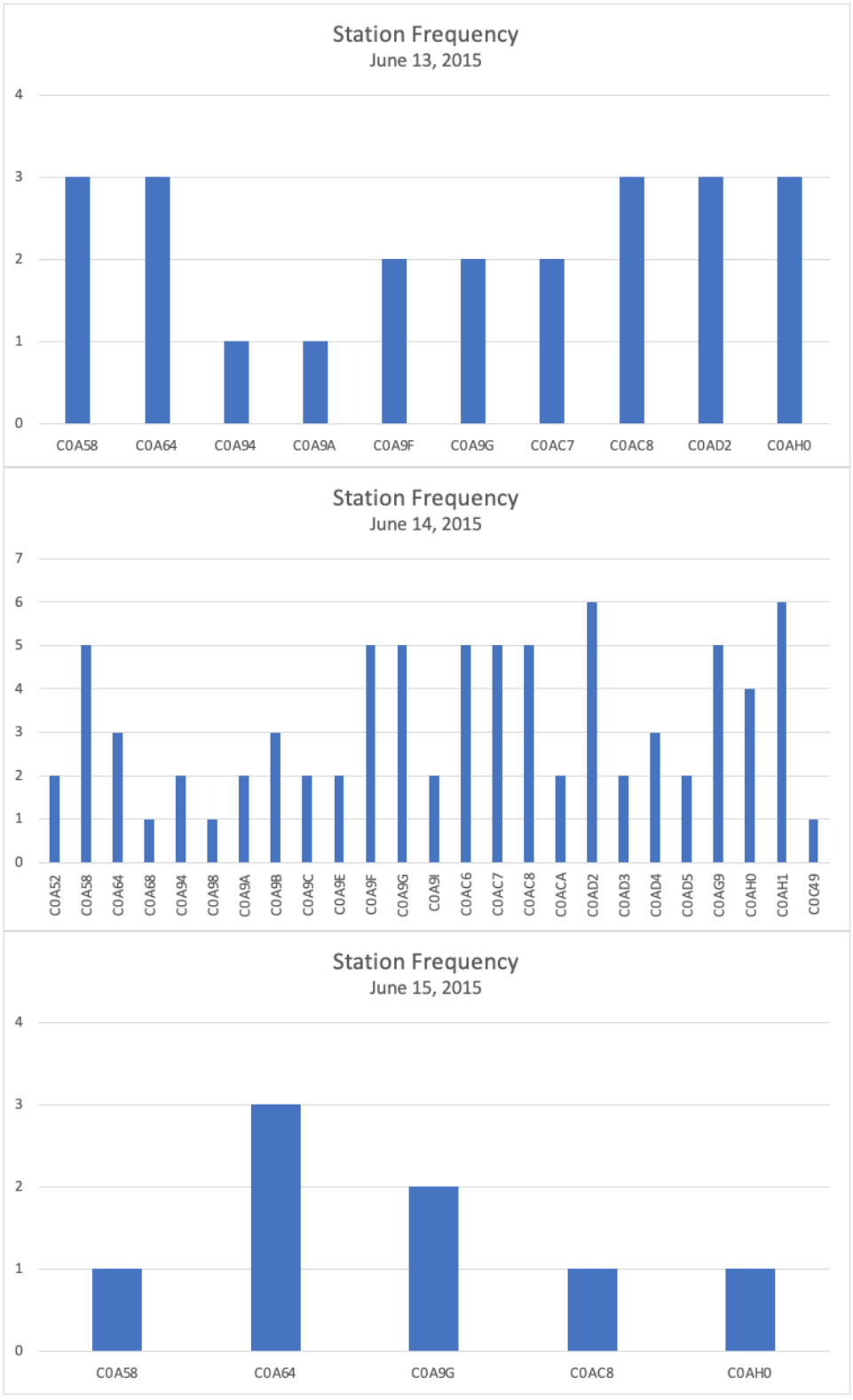

Figure 24: The stations recording rainfall and the total number of hours that rainfall was recorded at each station.

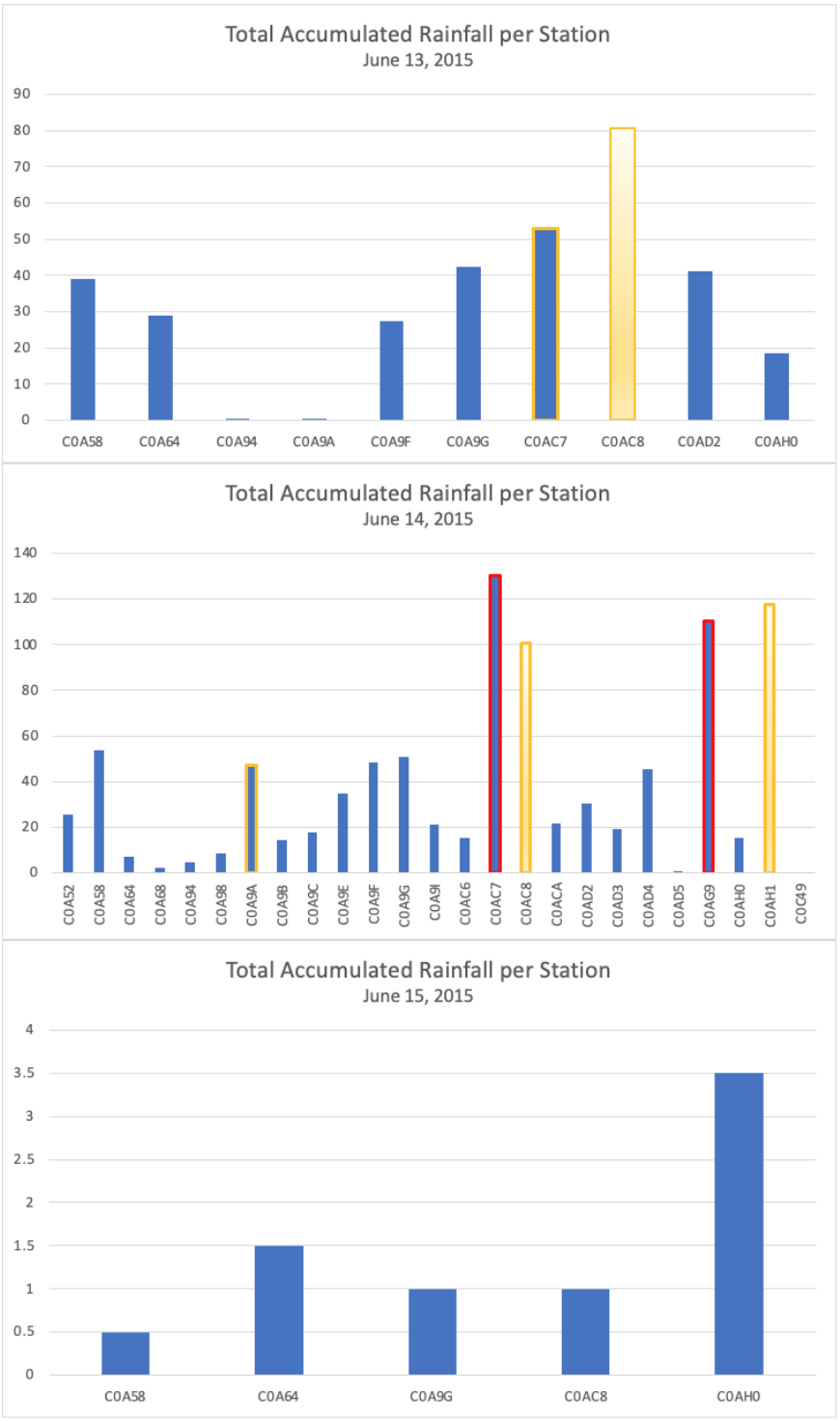

Figure 25: Total accumulated rainfall per station. A yellow outline means the 1-hr rainfall exceeds 40 mm, meeting the criteria for heavy rain advisory according to the CWB. A yellow fill means the 24-hr accumulated rainfall exceeds 80 mm, also meeting the criteria for a heavy rain advisory according to the CWB. A red outline means the 3-hr rainfall exceeds 100 mm, meeting the CWB criteria for an extremely heavy rain advisory.

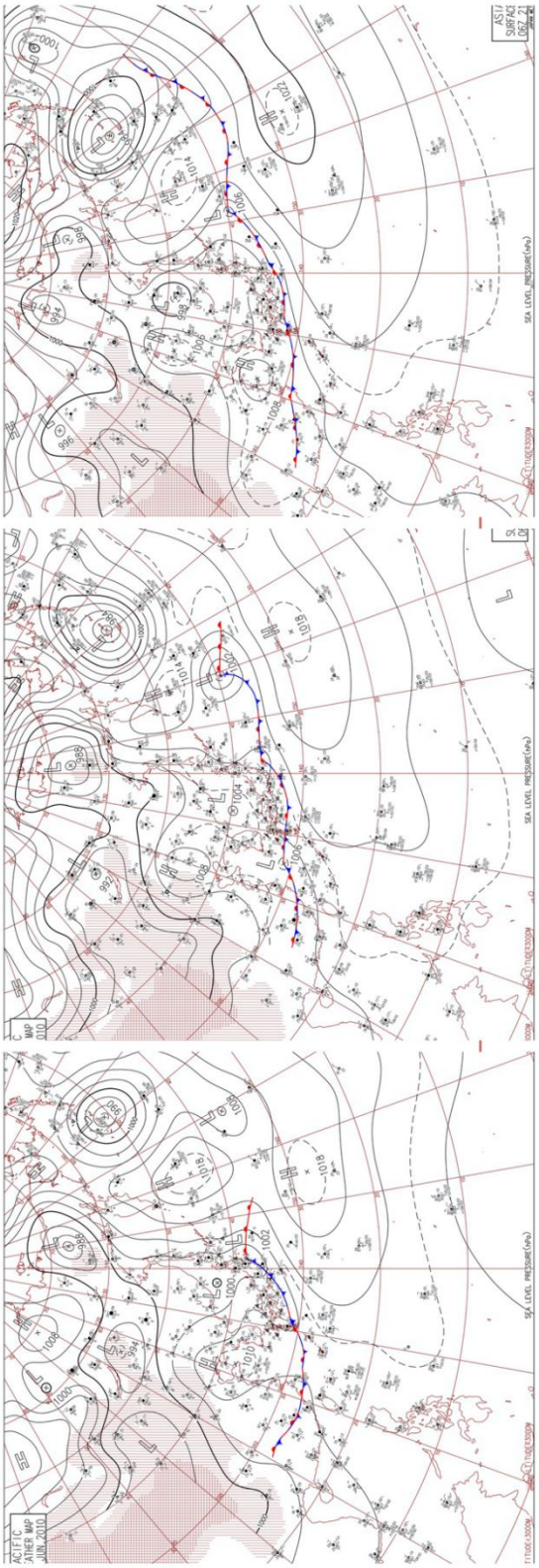

Figure 26: Surface analysis maps of June 21 – 23, 2010 courtesy of Japan Meteorological Society (Created by National Institute of Informatics "Digital Typhoon" based on "Weather Charts" from Japan Meteorological Agency)

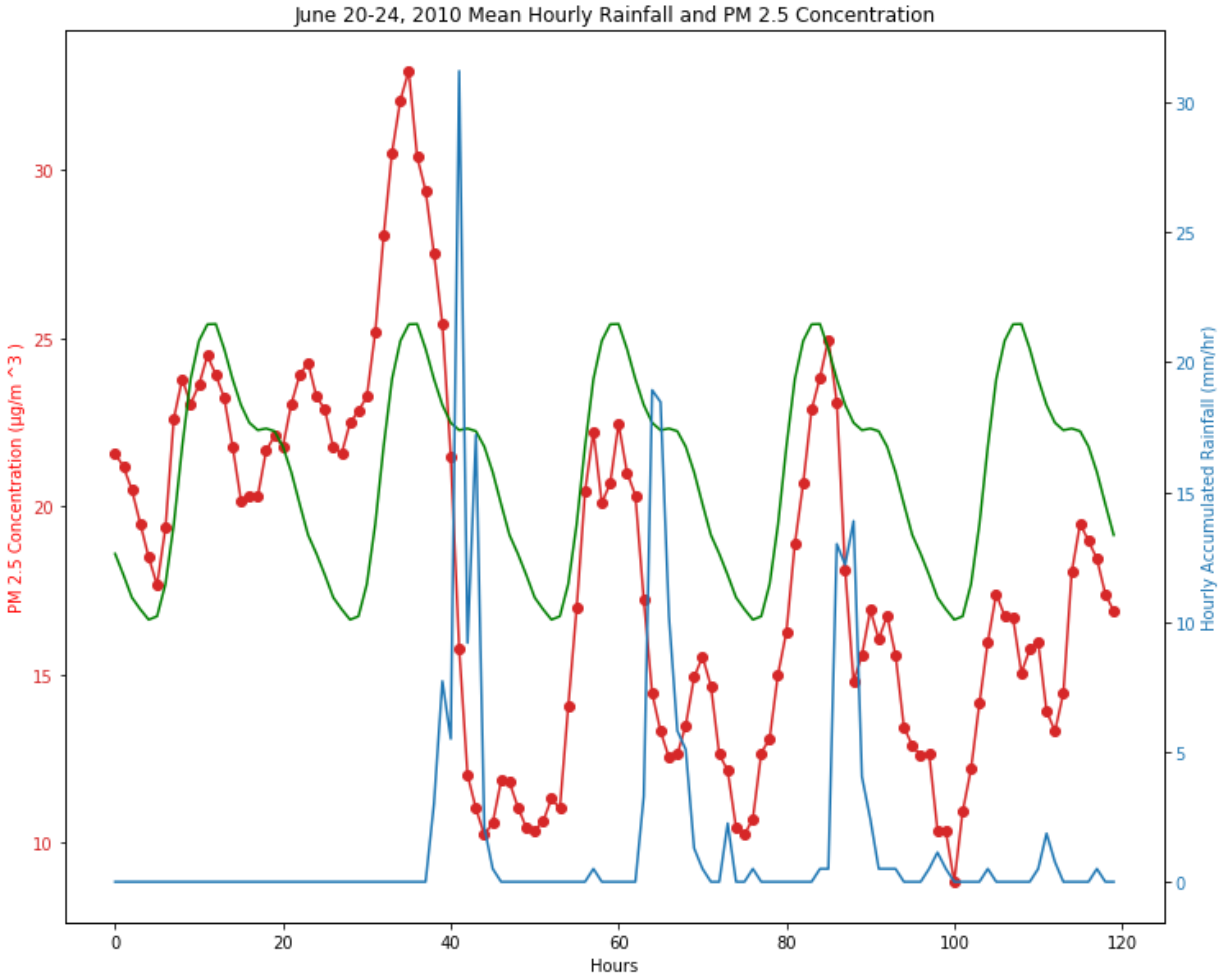

Figure 27: The hourly average PM2.5 concentration from June 20 to June 24, 2010 (red), the summer mean (green) and the accumulated hourly rainfall averaged across all the stations in the Taipei Basin (blue).

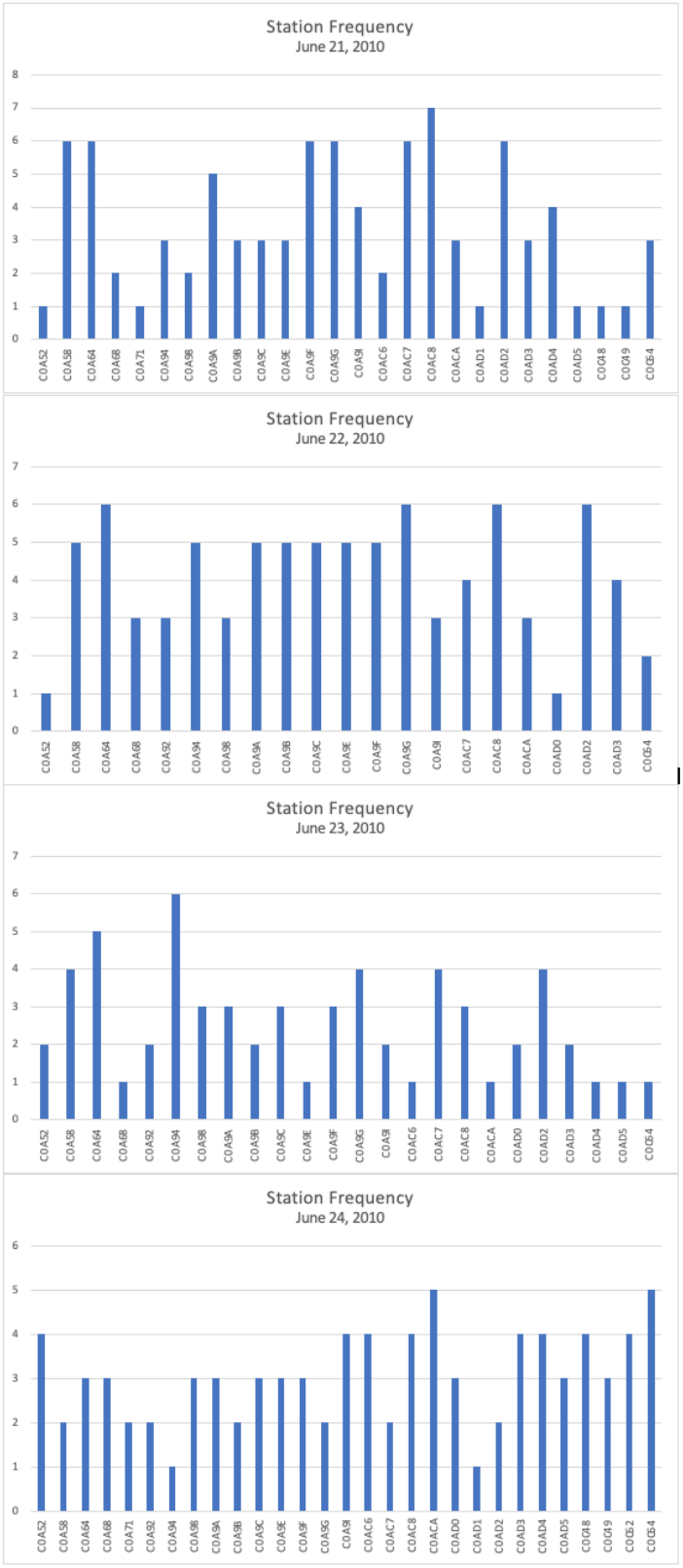

Figure 28: The stations recording rainfall and the total number of hours that rainfall was recorded at each station.

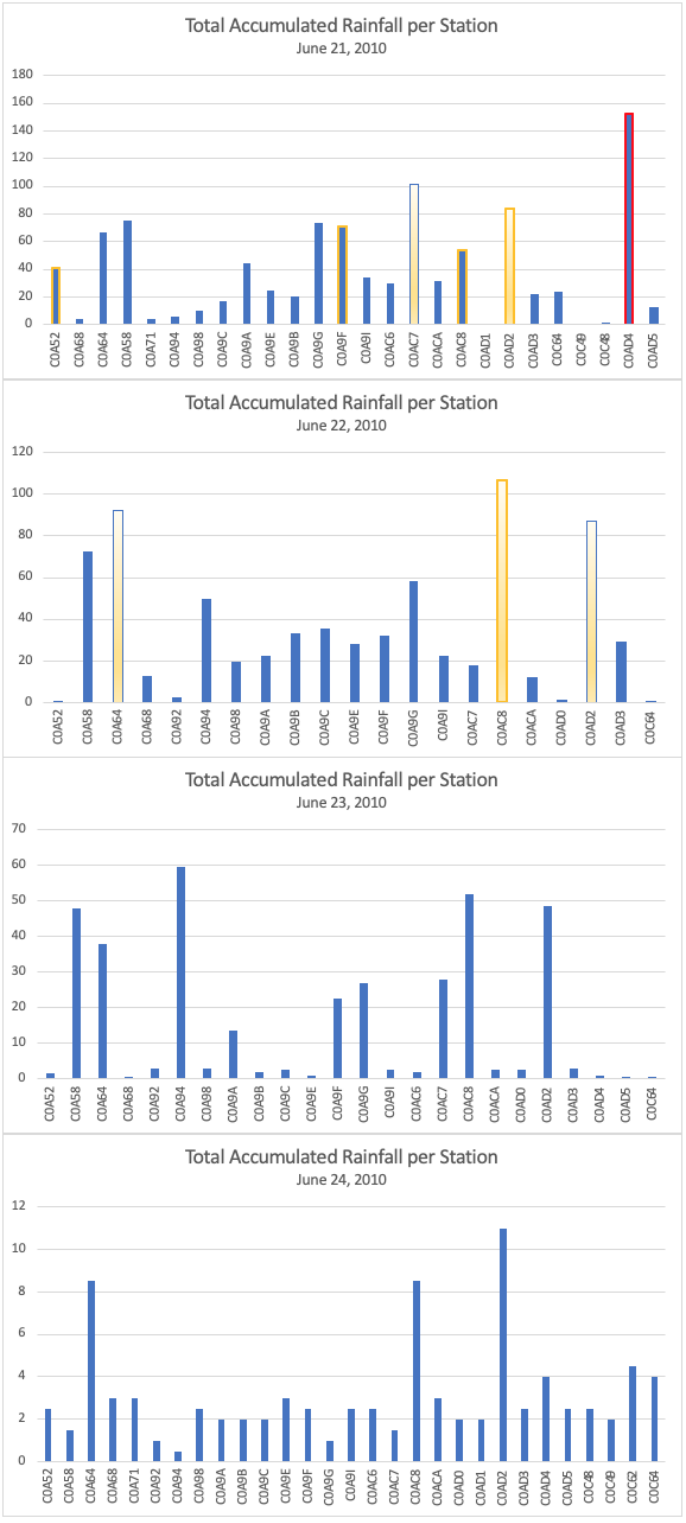

Figure 29: Total accumulated rainfall per station. A yellow outline means the 1-hr rainfall exceeds 40 mm, meeting the criteria for heavy rain advisory according to the CWB. A yellow fill means the 24-hr accumulated rainfall exceeds 80 mm, also meeting the criteria for a heavy rain advisory according to the CWB. A red outline means the 3-hr rainfall exceeds 100 mm, meeting the CWB criteria for an extremely heavy rain advisory.

5 Microphysics Sensitivity of Heavy Rain Events Under Varying PM2.5 Concentrations

Heavy rain events likely play a role in the observed PM2.5 trends. Aerosol concentrations may directly impact the development of heavy rain events. As discussed in Data and Methods (chapter 2), the July 5, 2007 thunderstorm was simulated at three different aerosol concentrations using the NTU version of the WRF-ARW model to determine whether aerosol concentrations influence heavy rainfall events. This specific storm was chosen as a representative case due to its synoptic similarity to the mean composite. The three concentrations were continental *clean*, continental *average*, and polluted *conditions*. In the simulations, the storm development, total precipitation, and rainfall rate were used as points of comparison.

5.1 Observation Information

The heavy rain event on July 5, 2007 is part of the DIRTY set of days described in section 2. This event was chosen because its synoptic environment closely resembles the pressure field composite shown in Figure 22. Specifically, a high-pressure system to the east and a low-pressure system to the west over the South China Sea. The radar observations of the storm show precipitation initiating over northern Taiwan, with precipitation recorded in the Taipei Basin at 15 LST. As the storm develops in the northern region, precipitation begins to extend further south to the remainder of the island (Figure 30).

5.2 Model Runs – Rainfall Totals

For all three model runs, precipitation began at 13 LST, two hours earlier than observations. In the model runs the rain lasted through to 16 LST. Figure 31 shows the rainfall accumulation over the period. There are notable differences between the three model runs, some observed as early as the first hour. Each column represents a different model run (*clean*, *average*, and *polluted*, respectively) and each row represents the total accumulated rainfall from 13 LST to

16 LST. In the *clean* run, there are two focus points. The same two focus points appear to be better connected in the *average* run. However, there is only one clear center point of precipitation in the *polluted* run. This single focus point trails down toward the southwest.

In all three runs, as the storm evolves, three main points of precipitation develop one in the north (A), one in the southwest (B), and one in the southeast (C) (Figure 31). The location points B and C are similar for all three runs; however, the concentrations vary. Point A varies in spatial extent and rainfall totals. In the *clean* run, point A appears to have two main points of precipitation, and in the *average* run, the focal point is located further to the northeast than the other two runs. There is also a difference between runs in the northeastern extent of precipitation from point B and in the southwestern extent from point A. Specifically, the *clean* run shows the rainfall more concentrated over point B, whereas the average and *polluted* runs show an extension towards point A. Point B has the largest difference in the second and third rows (hours 14 and 15 LST). A difference in rainfall amounts between runs is also observed. Specifically, rainfall accumulated in the *polluted* run by 15 LST (more than 100 mm) was substantially higher than the accumulated amounts in *clean* and *average*. Point C exhibited similar location, extent, and precipitation amounts in all three runs.

The difference in characteristics between A, B, and C reflect ways in which aerosol concentrations can impact rainfall distribution and storm development. By 16 LST *polluted* has a higher rainfall total with most of the rain located at point B, yet in a different manner than *clean* and *average*. Further analysis in the following section helps clarify if the rainfall rate and rainfall totals in *polluted* are in fact higher than the other two environments. It is possible that changes in the microphysical environment not only changes the microphysics of the storm itself but also how it interacts with the topography of the Basin.

5.3 Model Runs – Differences in Rainfall Patterns

To better delineate the differences in precipitation between different aerosol concentrations, the hourly rainfall totals were plotted from 12 to 15 LST (Figure 32). Points A, B, and C are located over the same region shown in Figure 31. However, there are more distinct rainfall patterns when looking at the hourly totals. The second row shows that most of the precipitation occurred between 13 and 14 LST for all three runs. The amounts, however, vary per run, with the *clean* run having the highest precipitation total over point C and the *average* and *polluted* runs having the highest precipitation total over point B.

The spatial distribution of this precipitation varies in the same ways described previously for Figure 31, with the *average* and *polluted* runs having less of a distinction between points A and B. The biggest difference in rainfall is seen in the third and fourth rows, where each run has unique characteristics. From 14 to 15 LST (third row), all three runs have most of the precipitation focused over point B with some light rainfall over point C and to the south of the basin. The *average* run has the lowest rainfall totals of the three runs, with most rainfall occurring over point C and some precipitation over the northeast part of the island beyond point A. The *clean* run has more rainfall over point B than the *average*, but neither the *clean* nor *average* runs have as high precipitation totals as the *polluted* run. The *polluted* run has considerable rainfall over point B relative to the other runs, with the heaviest precipitation falling over a slightly larger area than the previous hour. Unlike the initial hypothesis mentioned in previous chapters where it was thought that in a *clean* environment it would rain more and for a longer period, it turns out that there is more rain and a higher rainfall rate in a *polluted* environment. Point C records a similar amount of rainfall as the previous hour but over a much larger area. With the exception of some light precipitation to the southeast of the basin, there is

no rainfall in the *polluted* run, between 15 and 16 LST. The *average* run records more precipitation than it did in the previous hour over point C and in the southern end of the basin. The *clean* run also records precipitation in the southern end of the basin.

The precipitation maps in Figures 31 and 32 provide a qualitative assessment of the geographic extent of the storms and the varying rainfall amounts across the basin. It was found that more rain falls in a polluted environment (Figure 31 shows the rainfall totals) and there are differences in rainfall distribution, with a polluted environment having the majority of its rain fall over point B. Having point data, however, provides a better delineation of differences in rainfall duration and rainfall rates, especially to confirm if polluted has a higher rainfall rate. For this reason, the location of the rainfall observation stations was factored into the model coordinates and was used to create both station frequency and total accumulated rainfall graphs.

Figure 33 shows the hourly PM2.5 concentration, the PM2.5 summer mean, and hourly precipitation averaged across all stations in the basin. Unlike the previous hourly analysis plots where the hourly PM2.5 concentration has lower measurements than the summer mean, the PM2.5 concentration across the basin is always higher than the summer mean from July 4 to July 6. On July 4, the day before the heavy rain event, the hourly concentration follows a similar pattern to the summer mean. Not much rain is recorded, so there is no clear washout effect. On July 5, the heavy rain day, the PM2.5 concentration spikes about two hours before rainfall is recorded but does not decrease rapidly once rain begins. Unlike the other case studies, the PM2.5 concentration does not decrease rapidly or reach its lowest levels directly after heavy rain occurs. It is almost as if the rain has no washout effect on the existing PM2.5. On July 6, the day after the heavy rain event, PM2.5 concentrations were higher than the previous two days. The

concentration decreases about 10 µg/m^3 by the end of the day to reach the same concentration as July 5 but still higher than July 4.

5.4 Observation Station Frequency

Station frequency graphs (Figure 33) provide information on the duration of rainfall at a given point (observation station) and allow for determination of where rainfall was sustained the longest. In the observations of July 5, 2007 there was precipitation recorded at ten stations throughout the whole basin with an average rain duration of 2.1 hours. However, station C0A58 in the basin's south recorded precipitation for the longest (4 hours). These data were used as a comparison for the *clean*, *average*, and *polluted* runs. However, all three runs used the information from all stations that existed by 2015 (32 total stations) to maximize the data available for analysis. The clean run had seven (C0A52, C0A58, C0AC6, C0ACA, C0AD3, C0AD4, C0AD5) out of 27 stations precipitating for four hours. All seven stations are located in the southwest region of the basin. Since there was only rainfall in the basin for those four hours, that means that the southwestern part of the storm was able to sustain itself for the duration of the storm. On average, it rained for 2.78 hours, which is more than half an hour longer than the observations. The average model run had 25 stations precipitating for an average of 2.36 hours. Eleven of the 25 stations had rainfall for three hours.

These stations are located throughout the whole basin, not concentrated in a specific region like they were in the *clean* run. The *polluted* run recorded rainfall at only 22 stations, and only two stations (C0A9B, C0A9E) recorded rainfall for four hours. These two stations are located slightly north of the city center, where the PM2.5 emissions are generally the highest. This run had rainfall recorded for an average of 2.45 hours across the 22 stations. The duration of

rainfall provides further insight into where the rainfall could sustain itself the longest and where it passed through momentarily.

5.5 Observation Station Totals and Duration

Knowing the average rainfall duration for each run enables the determination of rainfall rates once the total rainfall amounts at each station (Figure 34) are analyzed. In the observations, most of the precipitation was concentrated at three stations (C0A52, C0A58, C0A9F). Station C0A52 is located southwest of the basin, C0A58 is located south of the basin, and C0A9F is east. The different locations of the stations throughout the basin show the widespread rainfall distribution and that the heaviest rain was not central to a single location. The total rainfall for the observations was 150.5 mm, which yields a relative average of 15.05 mm per station (150.5 mm / 10 observation stations). The relative average can be divided by the average number of hours that rained (2.1 hrs) to get the average relative rainfall rate per station: 7.17 mm/hr. The majority of the rainfall in the *clean* run occurred at station C0ACA for a total of 66.78 mm over the southwestern region of the basin. The total rainfall at the 27 station points recorded was 488.22 mm, more than three times the total from the observed measurements. However, in order to account for the difference in the number of stations (10 versus 27), the relative average is calculated to be 15.26 mm per station (488.22 mm / 27), which is similar to the observed relative average (0.21 mm difference). By dividing that average per station by the average number of hours precipitating (15.26 mm/ 2.78 hr), the relative rainfall rate of the *clean* run can be calculated to be 5.49 mm/hr, which is 1.68 mm/hr less than the observations. The *average* run had two main precipitation points, with C0AC8 being to the east of the basin and C0ACA being to the southwest. It is likely that these two stations fall in the region of points B and C and supports the idea that heavy precipitation was not concentrated to a single point. Further,

C0ACA meets the CWB criteria for a Heavy Rain Advisory by recording more than 40.00 mm in one hour. In total, all of the station points recorded 572.39 mm, which is divided by the 25 station points, gives a relative average of 17.89 mm per station. After considering the average rainfall duration in the *average* run (2.36 hr), the relative rainfall rate is 7.58 mm/hr (17.89 mm/ 2.36 hr), which is higher than both the observations and the *clean* run (by 0.41 mm/hr and 2.09 mm/hr, respectively).

The *polluted* run was very different from the other runs and the observations. A single station point (C0A52) recorded almost 112 mm in three hours, meeting the criteria for both a Heavy Rain Advisory (exceeding 80 mm in 24 hours) and an Extremely Heavy Rain Advisory (exceeding 100 mm in 3 hours). Both stations C0ACA and C0AD2 meet the CWB criteria for a Heavy Rain Advisory, signifying that the precipitation at these points was also substantial. Stations C0A52 and C0ACA are located near point B in the southwestern part of the basin, while station C0AD2 is closer to point C on the eastern side of the basin. A total of 622.71 mm was recorded at 22 station points, and the relative average was calculated to be 19.46 mm. Dividing it by the average duration of 2.45 hours, the average relative rainfall rate is 7.94 mm/hr making the *polluted* run have the highest rainfall rate.

5.6 Summary

In summary, the microphysics experiment using different aerosol concentrations shows that changes in the initial conditions trigger a shift in the location of the general rainfall and heavy rainfall centers. The changes in aerosols may therefore affect the microphysics development in the clouds and therefore, the convective evolution. The key points to take away from the microphysics modeling experiment are:

1. Changes in aerosol concentrations affects storm development, movement, interactions with topography, and rainfall rates.
2. Some of the changes in convective evolution are reflected in changes in the timing and distribution of the rain, most notably in the third row of Figure 32. In *average* conditions, the storms has basically dissipated, in *clean* the storm has weakened compared to the previous hour when the heaviest rain fell, but in *polluted* there is still heavy precipitation ongoing.
3. The rainfall rate *clean*: 5.49 mm/hr versus *polluted*: 7.94 mm/hr suggests that in a "clean" environment, the precipitation may last longer, but that does not necessarily mean more rain is falling. In contrast, in a "polluted" environment, there is a lot more rain falling in less time.

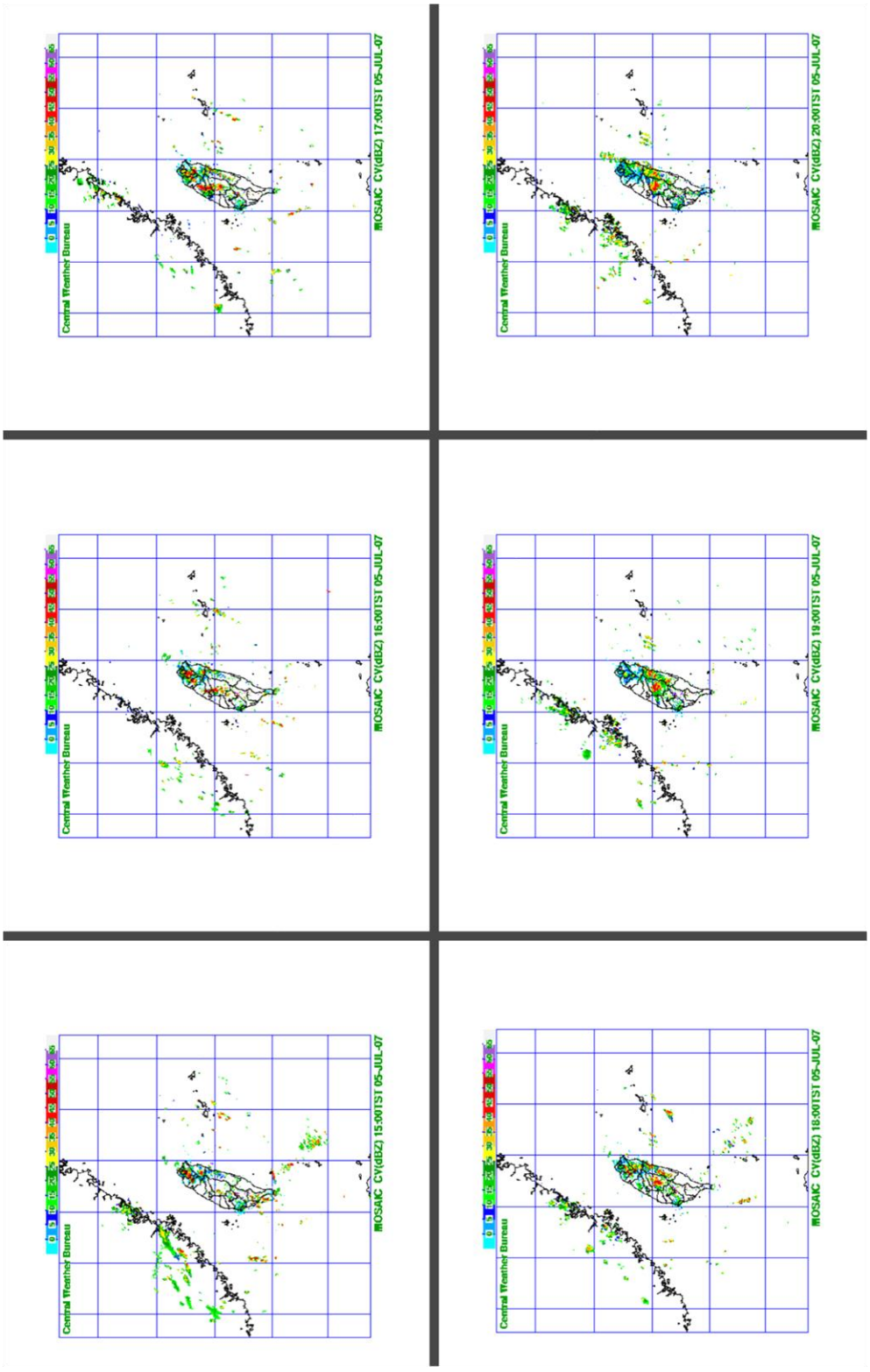

Figure 30: Hourly CWB radar images of July 5, 2007 from 15 to 20 LST.

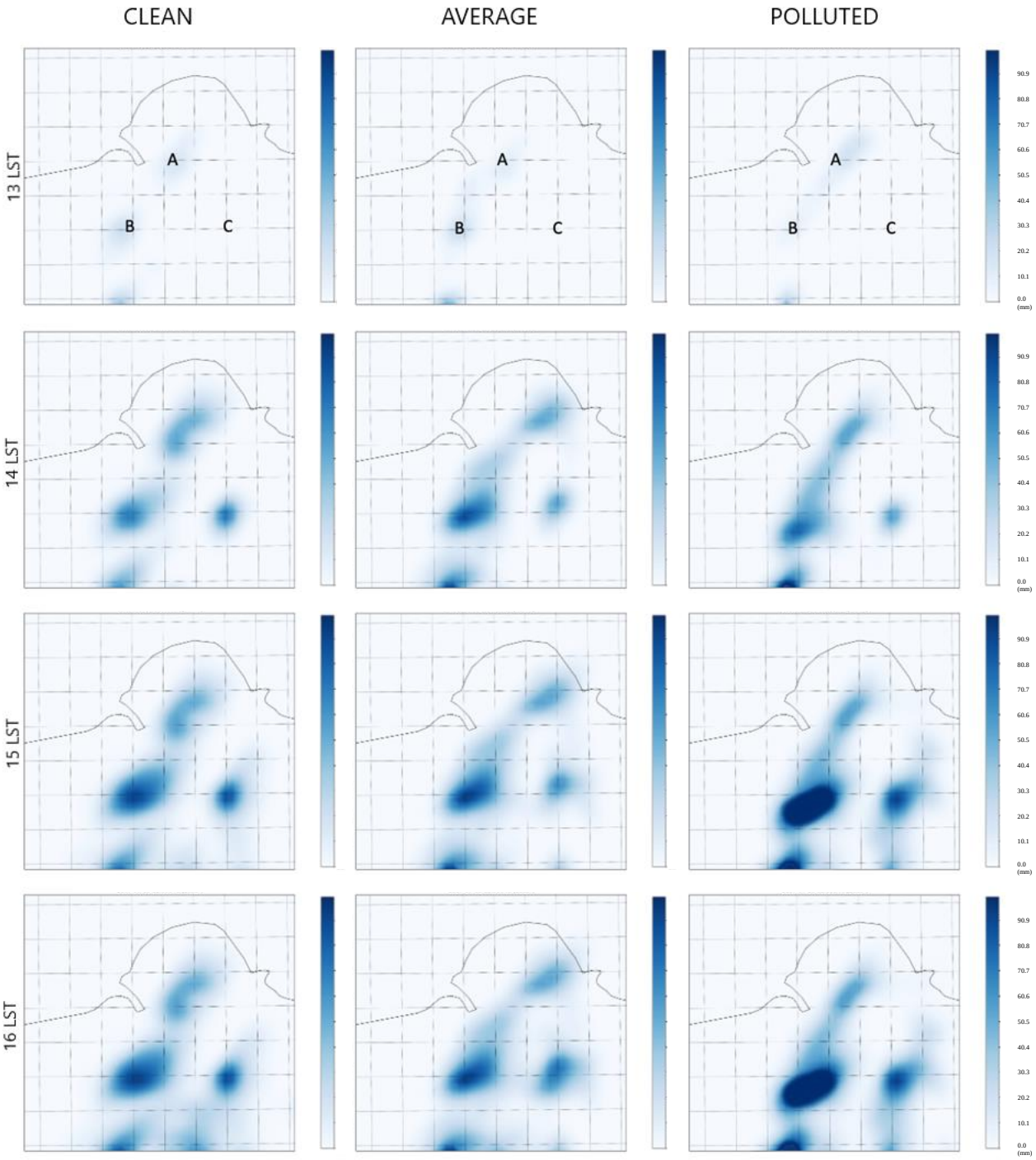

Figure 31: Total accumulation per hour over the Taipei Basin for each of the model runs from 13 to 16 LST.

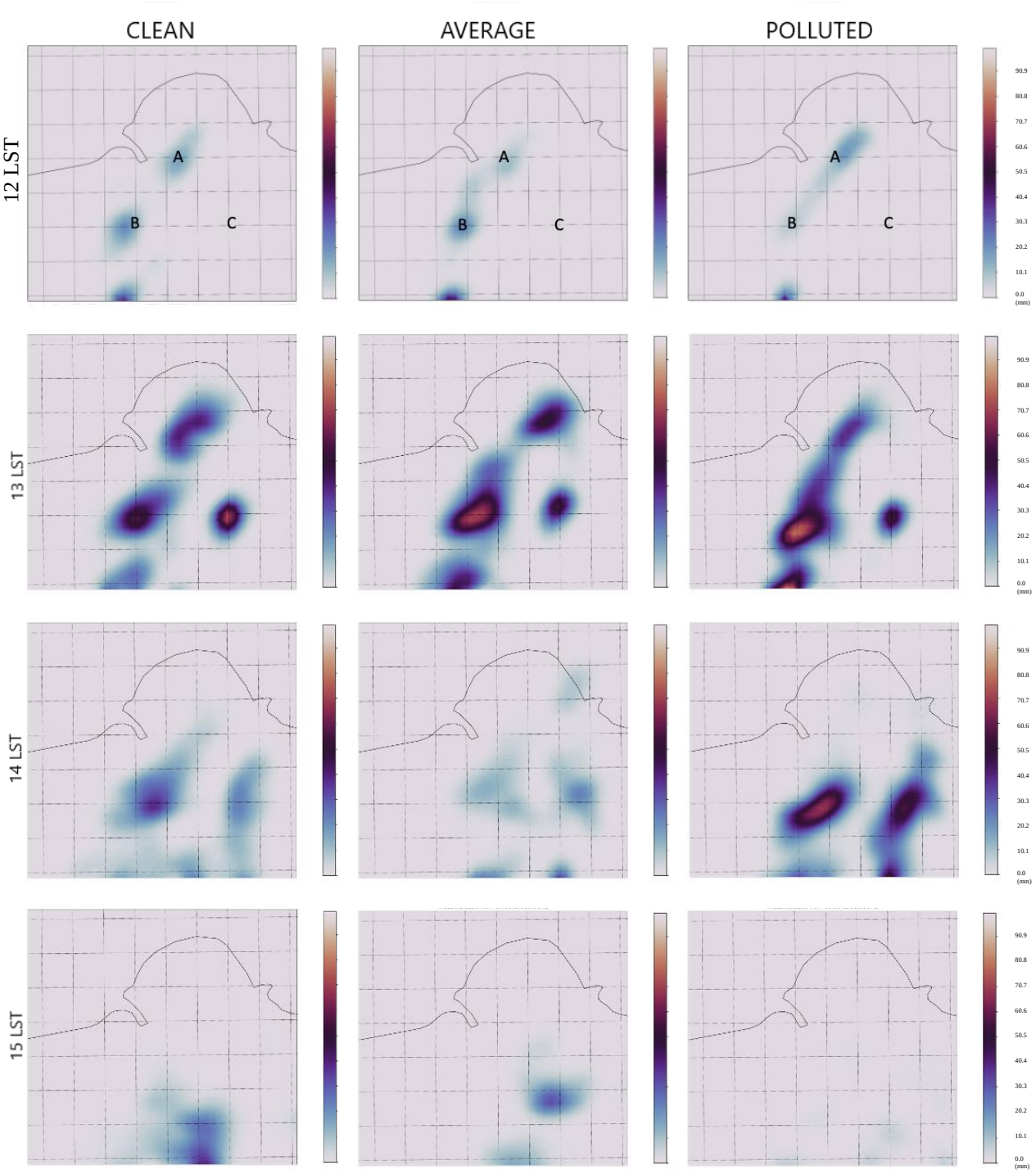

Figure 32: Hourly precipitation accumulation over the Taipei Basin for each of the model runs from 12 to 15 LST.

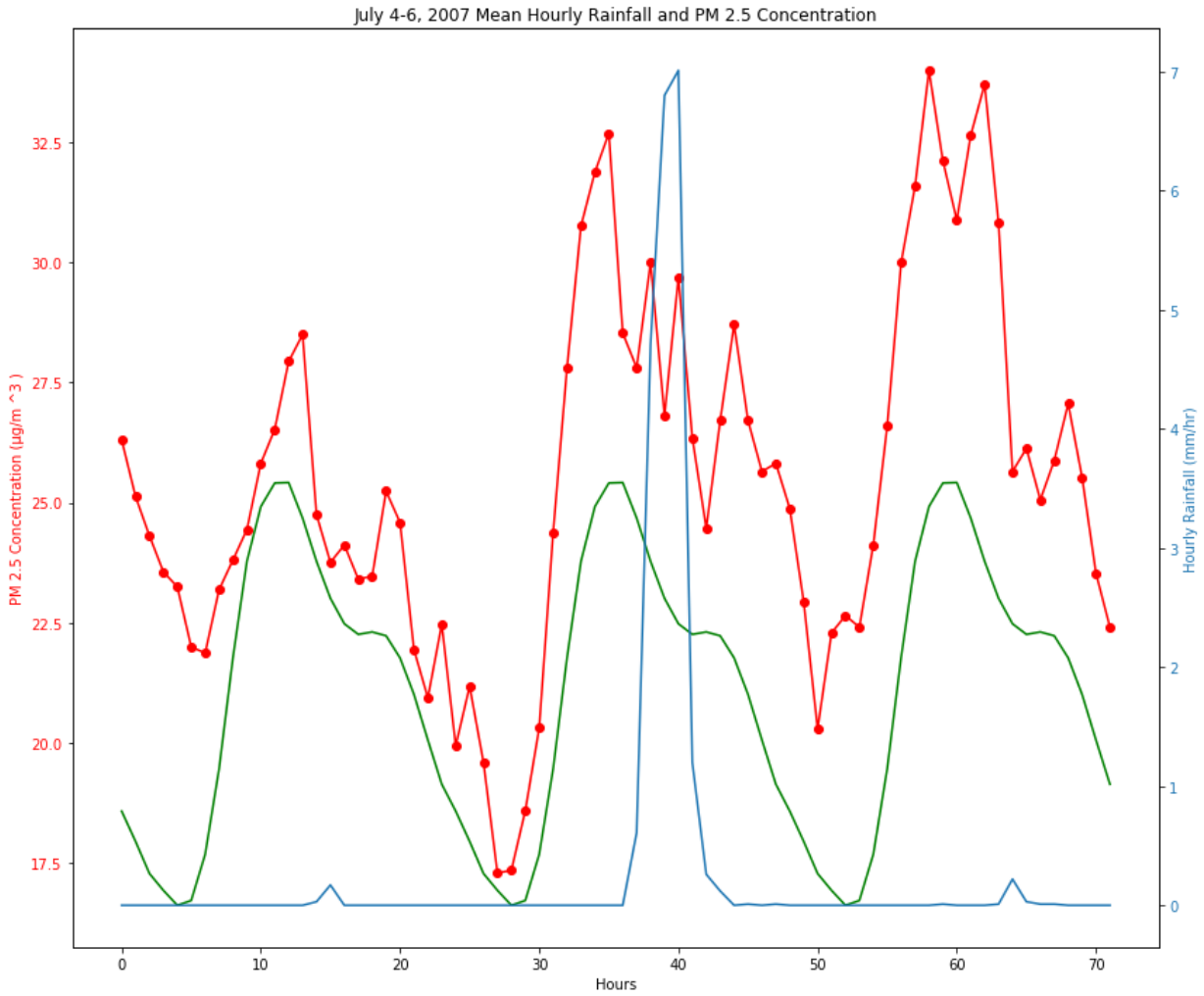

Figure 33: Hourly average PM2.5 concentration from July 4 to 6, 2007(red), the summer mean (green) and the accumulated hourly rainfall averaged across all the stations in the Taipei Basin (blue).

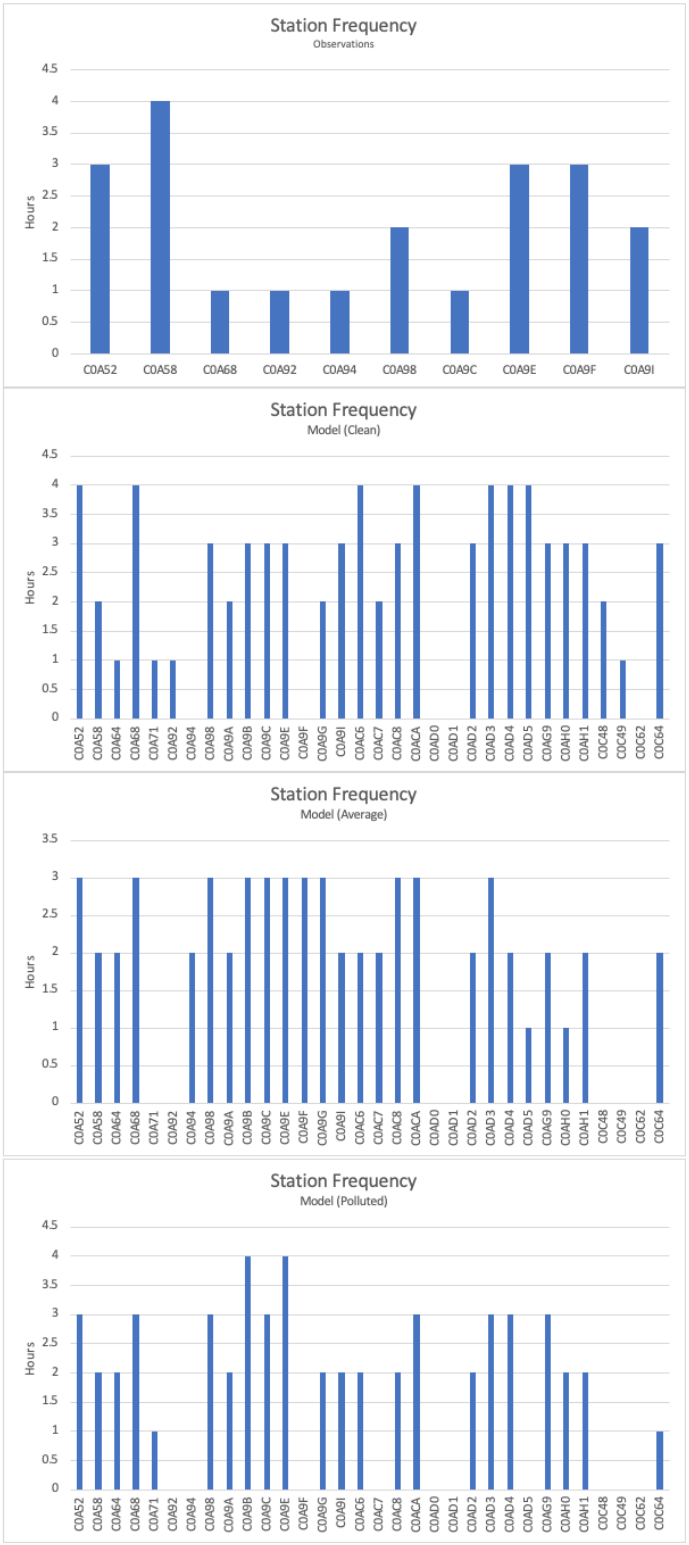

Figure 34: The stations recording rainfall and the total number of hours that rainfall was recorded at each station.

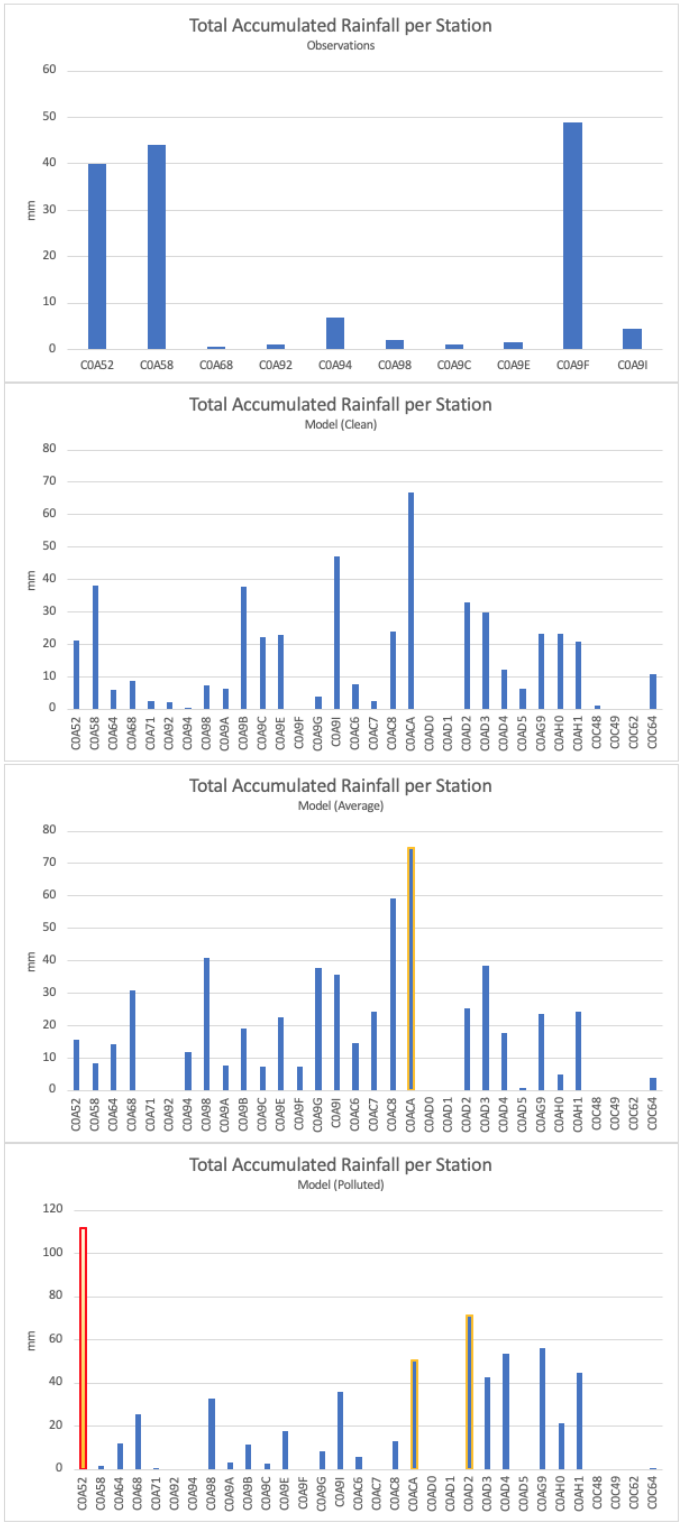

Figure 35: Total accumulated rainfall per station. A yellow outline means the 1-hr rainfall exceeds 40 mm, meeting the CWB criteria for heavy rain advisory. A yellow fill means the 24-hr accumulated rainfall exceeds 80 mm, meeting the CWB criteria for a heavy rain advisory. A red outline means that a 3-hr rainfall exceeds 100 mm, meeting the CWB criteria for an extremely heavy rain advisory.

6 Conclusions

This thesis is concerned with the trends in PM2.5 concentration over the Taipei Basin from 2005 to 2015 and their relation to heavy rainfall events in the same region. Adherence to EPA regulations decreased PM2.5 concentration by about 3 μg/m3 throughout the decade, but this did not seem to influence precipitation amounts. The heaviest rainfall events (top 5%) in June, July, and August were analyzed. The number of heavy rain events did not change. Rather, there seemed to be an increase in the amount of precipitation over time. However, there was still a lack of response in long-term precipitation to changes in PM2.5 concentrations. The lack of response motivated further examination of PM2.5 trends and heavy rain events to understand what the relationship is between PM2.5 and heavy rain events.

First, it was found that days without any precipitation have a higher PM2.5 concentration than heavy rain days due to the synoptic environment forcing strong subsidence. This conclusion came from analyzing surface weather maps of every heavy rain day and the days on the periphery. The heavy rain days/events were broken down into various groups to understand how precipitation responded differently to varying PM2.5 concentrations within the original set of days. Two sets of days, PRE and OTHER, had PM2.5 concentrations similar to the background summer mean. PRE refers to all the days directly before a heavy rain event, excluding days whose previous day was also a heavy rain event. OTHER refers to days whose mean PM2.5 concentration fell in the median range of all heavy rain days. POST days, which refers to days directly after a heavy rain event, had lower PM2.5 concentrations initially due to washout but recovered to background summer mean values by the end of the day. When the heavy rain events were separated based on concentration, CLEAN days had a stronger response to precipitation by having the PM2.5 concentration decrease by 5 μg/m3. This is compared to a 0.2 μg/m3 decrease

that DIRTY days had. It was initially hypothesized that the effects of washout would be greatest on days with high PM2.5 concentrations, but the observation analysis proved otherwise.

The case studies of heavy rain events gave further insight into the effects of precipitation on local scale PM2.5 concentrations – both temporally and spatially. Before heavy rain began, there was always a spike in PM2.5 concentration of about +10 µg/m3, followed by a sharp decline to about 10 µg/m3 as the rainfall washed out particulates in the air. Despite the sharp concentration decrease in the hours following the end of the rainfall event, the PM2.5 concentration was able to recover to values similar to those of the day before the rain or even to the background summer mean (21.02 µg/m3). However, these case studies were not sufficient to test whether PM2.5 concentrations directly affected the convective development of these large precipitation-producing events.

WRF model runs with different PM2.5 concentrations for the same storm showed different rainfall rates compared to observations (observed: 7.17mm/hr, *clean*: 5.49 mm/hr, *average*: 7.58 mm/hr, *polluted*: 7.94 mm/hr). The calculations lead to the conclusion that it may rain for a longer period in a clean environment, but that doesn't mean more rain will fall. On the other hand, in a polluted environment, it may rain for a shorter period, but more rain is falling in total. The key takeaway is that polluted conditions have a higher rainfall rate and total precipitation than any other circumstance. This is a conclusion that follows Alizadeh-Choobari's (2018) results: deep convection is fostered in a polluted environment, allowing for more precipitation.

7 Future Work

While the exact changes that the varying PM2.5 concentrations have on HR storm development are not explicitly known, it is clear that there are changes in the rainfall distribution and center-point locations. Further modeling analysis with different initial conditions (other HR events) and analysis of cloud condensation nuclei size distributions may provide further insight into how various PM2.5 concentrations can affect the microphysical development of precipitation over the Taipei Basin. More research can be done into PM2.5 distributions, HR event raindrop size distribution, and how changes in the microphysical environment of said storms can affect how the storms interact with topography, the Taipei UHI, and moisture influx from the river valleys.

Along the same lines, it would be interesting to do a more detailed analysis of how rainfall was distributed throughout the basin in each of the days studied. Rather than averaging rainfall totals, one can look at the specific time stations record rainfall and see how this can change the concluded relationship with PM2.5 and even the rainfall rates between *clean, average,* and *polluted*. There may even be unique characteristics across different parts of the basin (i.e., urban centers like Zhongshan and Sanchong versus a more distant Yangming).

It would also be worth looking into what the PM2.5-rain relationship looks like for storms that are not solely under weak synoptic forcing. Like the Mei-Yu case in Chapter 4, many summer afternoon storms also occur in a strong synoptic environment. Such storms under strong synoptic forcing would probably have similar results in a microphysics study but warrant a detailed study, nonetheless. A microphysics study could also delve into the likely suppression of warm rain happening for weak versus strong synoptic heavy rain days.

References

Ackerman, B., and Coauthors, 1978: *Summary of METROMEX, Volume 2: Cases of Precipitation Anomalies,* Bull. 63, Illinois States Water Survey, 395 pp.

Alizadeh-Choobari, O. Impact of aerosol number concentration on precipitation under different precipitation rates. *Meteorol Appl*. 2018; 25: 596– 605. https://doi.org/10.1002/met.1724

Baik, J.-J., Y.-H. Kim, J.-J. Kim, and J.-Y. Han, 2007: Effects of boundary-layer stability on urban heat island-induced circulation. Theor. Appl. Climatol., 89, 73-81.

Bornstein, R., and M. LeRoy, 1990: Urban barrier effects on convective and frontal thunderstorms. Extended Abstracts, Fourth Conf. Mesoscale Processes, Boulder, CO, Amer. Meteor. Soc., 120-121

Changnon, S. A., Jr., 1968: The La Ponte weather anomaly- Fact or fiction? *Bull. Amer. Meteor. Soc*., **49**, 4-11.

Changnon, S. A., Jr., F. A. Huff, P. T. Schickerdanz, and J. L. Vogel, 1977: *Summary of METROMEX, Volume 1: Weather Anomalies and Impacts.* Bull. 62, Illinois State Water Survey, 260 pp.

Chen, T., Tsay, J., & Takle, E. S. (2016). A Forecast Advisory for Afternoon Thunderstorm Occurrence in the Taipei Basin during Summer Developed from Diagnostic Analysis, *Weather and Forecasting*, *31*(2), 531-552. https://journals.ametsoc.org/view/journals/wefo/31/2/waf-d-15-0082_1.xml

Chen, T., Wang, S., & Yen, M. (2007). Enhancement of Afternoon Thunderstorm Activity by Urbanization in a Valley: Taipei, *Journal of Applied Meteorology and Climatology*, *46*(9), 1324-1340. https://journals.ametsoc.org/view/journals/apme/46/9/jam2526.1.xml

Chen, T., Yen, M., Tsay, J., Liao, C., & Takle, E. S. (2014). Impact of Afternoon Thunderstorms on the Land–Sea Breeze in the Taipei Basin during Summer: An Experiment, *Journal of Applied Meteorology and Climatology*, *53*(7), 1714-1738. **© American Meteorological Society. Used with permission.**
https://journals.ametsoc.org/view/journals/apme/53/7/jamc-d-13-098.1.xml

Cheng, C.-T., W.-C. Wang, and J.-P. Chen, 2007: A modeling study of aerosol impacts on cloud microphysics and radiative properties. *Quart. J. Roy. Meteor. Soc.*, **133**, 283–297, https://doi.org/10.1002/qj.25.

Cheng, C.-T., W.-C. Wang, and J.-P. Chen, 2010: Simulation of the effects of increasing cloud condensation nuclei on mixed-phase clouds and precipitation of a front system. *Atmos. Res.*, **96**, 461–476, https://doi.org/10.1016/j.atmosres.2010.02.005.

Chou, M. D., and M. J. Suarez, 1999: A solar radiation parameterization for atmospheric studies. *NASA Tech. Memo.* 104606, **15**, 40 pp.

Chou, M. D., M. J. Suarez, X. Z. Liang, and M. M. H. Yan, 2001: A thermal infrared radiation parameterization for atmospheric studies. *NASA Tech. Memo.*, 104606, **19**, 68 pp.

Craig, K. J., and R. D. Bornstein, 2002: MM5 simulations of urban induced convective precipitation over Atlanta. Preprints. Fourth Symp. on the Urban Environment, Norfolk, VA, Amer. Meteor. Soc., 5-6

Fuelberg, H. E., & Biggar, D. G. (1994). The Preconvective Environment of Summer Thunderstorms over the Florida Panhandle, *Weather and Forecasting*, *9*(3), 316-326. https://journals.ametsoc.org/view/journals/wefo/9/3/1520-0434_1994_009_0316_tpeost_2_0_co_2.xml

Han, Ji-Young & Baik, Jong-Jin & Lee, Hyunho. (2014). Urban impacts on precipitation. Asia-Pacific Journal of the Atmospheric Sciences. 50. 10.1007/s13143-014-0016-7.

Han, J. Y., J. J. Baik, and A.P. Khain, 2012: A numerical study of urban aerosol impacts on clouds and precipitation. *J. Atmos. Sci.* **69**, 504-520.

Hong, Song–You, Yign Noh, Jimy Dudhia, 2006: A new vertical diffusion package with an explicit treatment of entrainment processes. *Mon. Wea. Rev.*, **134**, 2318–2341. doi:10.1175/MWR3199.1

Hsu, C.H. and Cheng, F.Y. (2019). Synoptic Weather Patterns and Associated Air Pollution in Taiwan. *Aerosol Air Qual. Res.* 19: 1139-1151. https://doi.org/10.4209/aaqr.2018.09.0348

Kuo, K., & Wu, C. (2019). The Precipitation Hotspots of Afternoon Thunderstorms over the Taipei Basin: Idealized Numerical Simulations. *Journal of the Meteorological Society of Japan, 97*, 501-517.

Lin, C., Chen, W., Chang, P., & Sheng, Y. (2011). Impact of the Urban Heat Island Effect on Precipitation over a Complex Geographic Environment in Northern Taiwan, *Journal of Applied Meteorology and Climatology*, *50*(2), 339-353. https://journals.ametsoc.org/view/journals/apme/50/2/2010jamc2504.1.xml

Lin, C-Y., , F. Chen, , J. C. Huang, , W-C. Chen, , Y. A. Liou, , W. N. Chen, , and S. C. Liu, 2008b: Urban heat island effect and its impact on boundary layer development and land–sea circulation over northern Taiwan. *Atmos. Environ.*, **42 ,** 5639–5649.

Lin, P., Chang, P., Jou, B. J., Wilson, J. W., & Roberts, R. D. (2011). Warm Season Afternoon Thunderstorm Characteristics under Weak Synoptic-Scale Forcing over Taiwan Island, *Weather and Forecasting*, *26*(1), 44-60. https://journals.ametsoc.org/view/journals/wefo/26/1/2010waf2222386_1.xml

Miao, J.-E., and M.-J. Yang, 2020: A modeling study of the severe afternoon thunderstorm event at Taipei on 14 June 2015: The roles of sea breeze, microphysics, and terrain. *J. Meteor. Soc. Japan*, **98**, 129-152, doi: 10.2151/jmsj.2020-008.

National Institute of Informatics "Digital Typhoon" based on "Weather Charts" from Japan Meteorological Agency. http://agora.ex.nii.ac.jp/digital-typhoon/weather-chart/

Rosenfeld, D., Lohmann, U., Raga, G. B., O'Dowd, C. D., Kulmala, M., Fuzzi, S., Reissell, A., & Andreae, M. O. (2008). *Flood or drought: How do aerosols affect precipitation?*. Science | AAAS. https://www.science.org/doi/10.1126/science.1160606

Shepherd, J. M., Pierce, H., & Negri, A. J. (2002). Rainfall Modification by Major Urban Areas: Observations from Spaceborne Rain Radar on the TRMM Satellite, *Journal of Applied Meteorology*, *41*(7), 689-701. https://journals.ametsoc.org/view/journals/apme/41/7/1520-0450_2002_041_0689_rmbmua_2.0.co_2.xml

Taipei Population 2021 (Demographics, Maps, Graphs). (n.d.). Worldpopulationreview.com. https://worldpopulationreview.com/world-cities/taipei-population

Tewari, M., F. Chen, W. Wang, J. Dudhia, M. A. LeMone, K. Mitchell, M. Ek, G. Gayno, J. Wegiel, and R. H. Cuenca, 2004: Implementation and verification of the unified NOAH land surface model in the WRF model. *20th conference on weather analysis and forecasting/16th conference on numerical weather prediction*, pp. 11–15.

Tsai, T., & Chen, J. (2020). Multimoment Ice Bulk Microphysics Scheme with Consideration for Particle Shape and Apparent Density. Part I: Methodology and Idealized Simulation, *Journal of the Atmospheric Sciences*, *77*(5), 1821-1850. https://journals.ametsoc.org/view/journals/atsc/77/5/jas-d-19-0125.1.xml

US Department of Commerce, National Oceanic and Atmospheric Administration, National Weather Service, National Data Buoy Center. (2016). *NDBC - Science Education - What are sea breezes and why do they occur? - Answer*. Noaa.gov. https://www.ndbc.noaa.gov/educate/seabreeze_ans.shtml

US EPA. (2014, February 28). *Heat Island Effect*. US EPA. https://www.epa.gov/heatislands

US EPA. (2018, November 14). *Particulate Matter (PM) Basics | US EPA*. US EPA. https://www.epa.gov/pm-pollution/particulate-matter-pm-basics

Zhang, C. and Y. Wang, 2017: Projected Future Changes of Tropical Cyclone Activity over the Western North and South Pacific in a 20-km-Mesh Regional Climate Model. *J. Climate*, **30**, 5923-5941. doi:10.1175/JCLI-D-16-0597.1

Zhu, L., Meng, Z., Zhang, F., and Markowski, P. M. (2017). The influence of sea- and land-breeze circulations on the diurnal variability in precipitation over a tropical island, Atmos. Chem. Phys., 17, 13213–13232, https://doi.org/10.5194/acp-17-13213-2017